

Surface transverse linear momenta accompanying the reflection and refraction of a paraxial light beam

V. G. Fedoseyev*

Institute of Physics, University of Tartu, W. Ostwaldi 1, 50411 Tartu, Estonia

(Received 26 November 2018; published 20 May 2019)

The reflection and transmission of a paraxial light beam carrying the spin and intrinsic orbital angular momenta (IOAMs) at a plane interface between two isotropic transparent media is considered. The surface transverse linear momenta (STLMs), i.e., the momenta that are localized near the interface and whose direction is perpendicular to the plane of incidence, are investigated. The IOAM-dependent and spin-dependent STLMs of the beams of homogeneous and inhomogeneous plane waves as well as the interference STLMs in the first medium are calculated. A detailed comparison of these STLMs is made. The way of experimental investigation of STLMs based on the relation between the global STLM and the transverse shift of the center of gravity of the global electromagnetic field is discussed.

DOI: [10.1103/PhysRevA.99.053827](https://doi.org/10.1103/PhysRevA.99.053827)

I. INTRODUCTION

The purpose of the present paper is to investigate electromagnetic transverse linear momentum (TLM), which can be generated during reflection and transmission of a paraxial light beam at a plane interface between two isotropic homogeneous and transparent media. The term “transverse” denotes the direction perpendicular to the plane of incidence.

In the main part of the paper, LM defined in the sense of Abraham is considered. It is assumed that the light velocity in vacuum is equal to unity. Under such an assumption, the density of the Abraham LM is equal to the Poynting vector (see, e.g., [1]); as a consequence, TLM per unit length in the transverse direction is equal to the transverse power flow (TPF) of the electromagnetic energy that is generated in the course of the aforementioned process.

As for TPF, its investigation has a long and dramatic history. Already a century ago, TPF inside the evanescent field generated in the reflecting medium at total reflection of a plane wave was calculated [2]. Later it was shown that such a TPF occurs when the evanescent plane wave is elliptically polarized [3,4]. It has also been pointed out that the appearance of such a TPF is connected to transformation of the spin at reflection and transmission of the plane wave [5]. Therefore, TPFs as well as TLMs depending on the polarization of the incident wave (more generally, on the polarization of the incident beam) will be called the spin-dependent ones.

Initially it was believed that the generation of the spin-dependent TPF is inseparable from the generation of inhomogeneous (evanescent) waves in the reflecting medium that takes place at total reflection or at reflection from a lossy medium [2–7]. However, it was later shown that the spin-dependent TPFs of the incident, reflected, and transmitted homogeneous plane waves can also occur [8], their values being of the same order of magnitude as the values of TPF inside the evanescent field. Again, the interference TPF in

the first medium can also be of the same order of magnitude [8,9].

Besides spin, the beam of electromagnetic waves can also carry an intrinsic orbital angular momentum (IOAM) [10]. The latter is now of significant interest; a number of papers have been devoted to the investigation of IOAM and IOAM-dependent phenomena; see, e.g., [11–13]. In the present paper the calculations of the IOAM-dependent TLMs generated during reflection and transmission of a light beam are carried out. For the sake of completeness, the spin-dependent TLMs are also considered, and the comparison of two TLMs is made.

TLMs confined in the domains adjacent to the interface whose dimensions are large in comparison with the incident beam’s width are calculated. They are divided into the parts that are independent of and dependent on the domains’ dimensions. The former TLMs, which are called the surface TLMs and denoted as STLMs, are investigated in detail. As for the latter TLMs, the conditions are clarified under which these can be ignored when investigating STLMs.

The particular IOAM-dependent and spin-dependent STLMs of the beams of homogeneous and inhomogeneous plane waves as well as the interference STLMs in the first medium are calculated. STLMs in the incident and reflecting media as well as STLMs in the total space are also considered. It can be said that the complete investigation of STLMs that can be generated under the aforementioned conditions imposed on the incident beam and on the media is carried out in this paper. The TPF phenomenon is also discussed.

Only such STLMs are investigated in detail whose values are independent of the incident beam’s width and are left finite as the width tends to infinity. The scale of these STLMs is LM confined in the sector of the incident beam whose length is $(2\pi)^{-1}$ times the wavelength. It is shown that all aforementioned particular spin-dependent STLMs but only the particular IOAM-dependent STLMs of the beams of homogeneous plane waves can be on such a scale. The explanation of such a distinction between the spin-dependent and IOAM-dependent STLMs is given.

*fedo@fi.tartu.ee

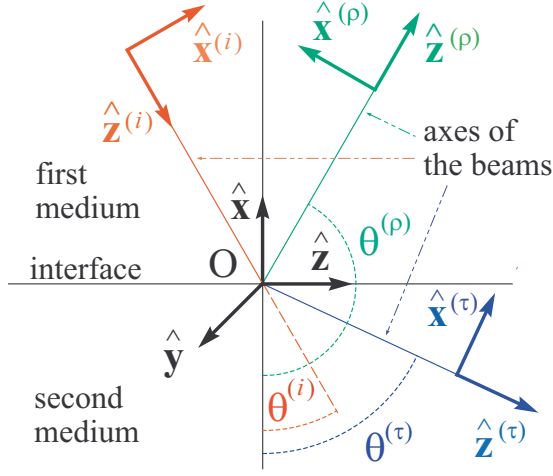


FIG. 1. Geometry of reflection and transmission. The characteristics of the incident, reflected, and transmitted beams are represented in red, green, and blue, respectively. $n^{(1)} > n^{(2)}$, $\theta^{(i)} < \theta^{(iC)}$.

The geometrical interpretation of the particular IOAM-dependent STLMS is presented.

It was pointed out long ago that the appearance of TPF in the reflecting medium should lead to the transverse shift (TSh) of the totally reflected light beam [3,4,6,7,9]. In [14,15] the general relation between the global Abraham TLM and TSh of the center of gravity (TShCG) of the global secondary field has been established. On the basis of such a relation, in this paper the possibility of the experimental investigation of the spin-dependent and IOAM-dependent STLMS through measuring respective TShCGs of secondary beams is discussed. Note that the TSh phenomenon has been intensively studied during the last decades; see, e.g., the review article [16] and the references therein.

In the end of the body of the paper, STLMS defined in the sense of Minkowski are considered, and the comparison of these STLMS with Abraham ones is made. The distinction between the Abraham and Minkowski STLMS is discussed from the point of view of the Abraham-Minkowski dilemma; for the latter, see, e.g., the review articles [17–20].

II. GEOMETRY OF REFLECTION AND TRANSMISSION

Let us consider the reflection and transmission of a monochromatic paraxial light beam at a plane interface between two semi-infinite transparent, isotropic, nondispersive, and nonmagnetic media. The scheme of this process is shown in Fig. 1.

Throughout the paper, the superscripts i , ρ , and τ will be used in order to label the characteristics of the incident, reflected, and transmitted beams, respectively. The superscripts a or a' will label the characteristic of an arbitrary beam, i.e., $a \in \{i, \rho, \tau\}$ and $a' \in \{i, \rho, \tau\}$. The superscript α will label the characteristics of secondary beams, i.e., $\alpha \in \{\rho, \tau\}$.

The dielectric constants of the first (upper in Fig. 1) and of the second media will be denoted by $\epsilon^{(1)}$ and $\epsilon^{(2)}$, respectively. We will also use the notation $\epsilon^{(a)}$ for the dielectric constant of the medium in which the a th beam propagates; i.e., we will assume that $\epsilon^{(i)} = \epsilon^{(\rho)} = \epsilon^{(1)}$ and $\epsilon^{(\tau)} = \epsilon^{(2)}$. The refractive

indices of the first and of the second media will be denoted by $n^{(1)}$ and $n^{(2)}$, respectively; $n^{(1,2)} = \sqrt{\epsilon^{(1,2)}}$.

The position of the interface is defined by the equation $\hat{\mathbf{x}} \cdot \mathbf{r} = 0$, where \mathbf{r} is a 3D radius vector, and $\hat{\mathbf{x}}$ is the unit normal to the interface. Four Cartesian frames will be employed. Three frames are attached to the incident, reflected, and transmitted beams, and the last one will be in use when considering the partial reflection. The basis of the a th frame is given by the unit vectors $\hat{\mathbf{x}}^{(a)}$, $\hat{\mathbf{y}}$, and $\hat{\mathbf{z}}^{(a)}$, which are defined below.

The $z^{(i)}$ axis is assumed to coincide with the incident beam's axis; its rigorous definition will be given later. The $z^{(i)}$ axis and the vector $\hat{\mathbf{x}}$ define the orientation of the beam's plane of incidence. The angle between $-\hat{\mathbf{x}}$ and $\hat{\mathbf{z}}^{(i)}$ is the beam's angle of incidence $\theta^{(i)}$; see Fig. 1. $\theta^{(i)} = -\arccos(\hat{\mathbf{x}} \cdot \hat{\mathbf{z}}^{(i)})$. We will consider the partial-reflection as well as the total-reflection regimes. The latter takes place if $n^{(2)} < n^{(1)}$ and $\theta^{(i)} > \theta^{(iC)}$, where $\theta^{(iC)} = \arcsin(n^{(2)}/n^{(1)})$ is the critical angle for total reflection; in this case the inhomogeneous (evanescent) plane waves are generated in the second medium.

The y axis (the transverse one) is common for all frames; it is perpendicular to the plane of incidence and is characterized by the unit vector $\hat{\mathbf{y}} = \hat{\mathbf{z}}^{(i)} \times \hat{\mathbf{x}} / |\hat{\mathbf{z}}^{(i)} \times \hat{\mathbf{x}}|$. The coordinate origin O in every frame is taken to be the point of intersection of the $z^{(i)}$ axis with the interface.

The $z^{(\rho)}$ and $z^{(\tau)}$ axes, whose directions are characterized by the unit vectors $\hat{\mathbf{z}}^{(\rho)}$ and $\hat{\mathbf{z}}^{(\tau)}$, will be assumed to coincide with the geometric-optical axes of the reflected and transmitted beams. They are defined as the rays that are intersected by the interface at the coordinate origin. $\theta^{(\rho)}$ and $\theta^{(\tau)}$ are the angles of reflection and refraction; see Fig. 1. $\theta^{(\rho)} = \pi - \theta^{(i)}$, while $\theta^{(\tau)}$ is defined by the relation $n^{(2)} \sin \theta^{(\tau)} = n^{(1)} \sin \theta^{(i)}$.

Every $x^{(a)}$ axis lies in the plane of incidence; its direction is given by the unit vector $\hat{\mathbf{x}}^{(a)} = \hat{\mathbf{y}} \times \hat{\mathbf{z}}^{(a)}$.

In the frame attached to the a th beam, 3D radius vector \mathbf{r} can be written as

$$\mathbf{r} = \mathbf{r}_p^{(a)} + z^{(a)} \hat{\mathbf{z}}^{(a)}, \quad (1)$$

where $\mathbf{r}_p^{(i)}$, $\mathbf{r}_p^{(\rho)}$, and $\mathbf{r}_p^{(\tau)}$ are 2D planar radius vectors lying in the planes perpendicular to the axis of the incident beam or to the geometric-optical axis of the respective secondary beam,

$$\mathbf{r}_p^{(a)} = x^{(a)} \hat{\mathbf{x}}^{(a)} + y \hat{\mathbf{y}}. \quad (2)$$

The fourth frame is attached to the interface; its basis is $\hat{\mathbf{x}}$, $\hat{\mathbf{y}}$, and $\hat{\mathbf{z}} = \hat{\mathbf{x}} \times \hat{\mathbf{y}}$.

III. THE ELECTROMAGNETIC FIELDS OF THE INCIDENT, REFLECTED, AND TRANSMITTED BEAMS

The complex amplitudes of electric and magnetic field vectors in the a th beam will be denoted by $\mathbf{E}^{(a)}(\mathbf{r})$ and $\mathbf{H}^{(a)}(\mathbf{r})$; their harmonic time dependence will be suppressed. Let us represent these vectors as superpositions of plane waves,

$$\mathbf{E}^{(a)}(\mathbf{r}) = \frac{1}{2\pi} \int \mathcal{E}^{(a)}(\boldsymbol{\kappa}) \exp[-i\mathbf{k}^{(a)}(\boldsymbol{\kappa}) \cdot \mathbf{r}] d^2\boldsymbol{\kappa}, \quad (3)$$

$$\mathbf{H}^{(a)}(\mathbf{r}) = \frac{1}{2\pi} \int \mathcal{H}^{(a)}(\boldsymbol{\kappa}) \exp[-i\mathbf{k}^{(a)}(\boldsymbol{\kappa}) \cdot \mathbf{r}] d^2\boldsymbol{\kappa}, \quad (4)$$

where $\mathbf{k}^{(a)}(\boldsymbol{\kappa})$ is the 3D wave vector of the particular plane wave in the a th beam, $\mathcal{E}^{(a)}(\boldsymbol{\kappa})$ and $\mathcal{H}^{(a)}(\boldsymbol{\kappa})$ are the electric and magnetic amplitudes of this wave, and $\boldsymbol{\kappa}$ is a 2D variable vector.

The wave vectors of the plane waves in the a th beam. Every wave vector $\mathbf{k}^{(a)}(\boldsymbol{\kappa})$ is related to $\mathbf{k}^{(i)}(\boldsymbol{\kappa})$ as follows: $\mathbf{k}^{(\rho)}(\boldsymbol{\kappa}) = \mathbf{k}^{(i)}(\boldsymbol{\kappa}) - 2[\hat{\mathbf{x}} \cdot \mathbf{k}^{(i)}(\boldsymbol{\kappa})]\hat{\mathbf{x}}$, while $\mathbf{k}^{(\tau)}(\boldsymbol{\kappa})$ can be expressed through $\mathbf{k}^{(i)}(\boldsymbol{\kappa})$ by means of Snell's law.

Let us denote by Λ the reverse wave vector of the incident plane wave,

$$\Lambda = \lambda/2\pi, \quad (5)$$

where λ is the wavelength of light in the first medium. Then $[\mathbf{k}^{(a)}(\boldsymbol{\kappa})]^2 = (\epsilon^{(a)}/\epsilon^{(1)})\Lambda^{-2}$. The direction of $\mathbf{k}^{(a)}(\boldsymbol{\kappa})$ can be characterized by the vector

$$\mathbf{z}^{(a)}(\boldsymbol{\kappa}) = (n^{(1)}/n^{(a)})\Lambda\mathbf{k}^{(a)}(\boldsymbol{\kappa}). \quad (6)$$

The vectors $\mathbf{z}^{(i)}(\boldsymbol{\kappa})$ and $\hat{\mathbf{x}}$ define the orientation of the plane of incidence for the particular plane wave. The unit vector perpendicular to this plane is as follows:

$$\hat{\mathbf{y}}(\boldsymbol{\kappa}) = \frac{\mathbf{z}^{(i)}(\boldsymbol{\kappa}) \times \hat{\mathbf{x}}}{|\mathbf{z}^{(i)}(\boldsymbol{\kappa}) \times \hat{\mathbf{x}}|}. \quad (7)$$

The vector $\mathbf{x}^{(a)}(\boldsymbol{\kappa})$ is parallel to the plane of incidence of the particular plane wave and orthogonal to $\mathbf{z}^{(a)}(\boldsymbol{\kappa})$; it is

$$\mathbf{x}^{(a)}(\boldsymbol{\kappa}) = \hat{\mathbf{y}}(\boldsymbol{\kappa}) \times \mathbf{z}^{(a)}(\boldsymbol{\kappa}). \quad (8)$$

The vectors $\mathbf{z}^{(i)}(\boldsymbol{\kappa})$ [$\mathbf{x}^{(i)}(\boldsymbol{\kappa})$] and $\mathbf{z}^{(\rho)}(\boldsymbol{\kappa})$ [$\mathbf{x}^{(\rho)}(\boldsymbol{\kappa})$], as well as $\mathbf{z}^{(\tau)}(\boldsymbol{\kappa})$ [$\mathbf{x}^{(\tau)}(\boldsymbol{\kappa})$] in the partial-reflection regime, are real; these are the unit vectors. Further on, when only these vectors are under consideration, they will be labeled by the "hat" symbol ($\hat{\cdot}$). In the total-reflection regime the vectors $\mathbf{z}^{(\tau)}(\boldsymbol{\kappa})$ and $\mathbf{x}^{(\tau)}(\boldsymbol{\kappa})$ are complex. In both regimes $[\mathbf{z}^{(a)}(\boldsymbol{\kappa})]^2 = [\mathbf{x}^{(a)}(\boldsymbol{\kappa})]^2 = 1$.

Let us assume that the wave vector $\mathbf{k}^{(i)}(0)$ is directed along the axis of the incident beam; then $\hat{\mathbf{z}}^{(i)}(0) = \hat{\mathbf{z}}^{(i)}$, $\hat{\mathbf{z}}^{(\rho)}(0) = \hat{\mathbf{z}}^{(\rho)}$, and, at partial reflection, $\hat{\mathbf{z}}^{(\tau)}(0) = \hat{\mathbf{z}}^{(\tau)}$ as well. Every vector $\mathbf{k}^{(a)}(\boldsymbol{\kappa})$ can be represented as follows:

$$\mathbf{k}^{(a)}(\boldsymbol{\kappa}) = \mathbf{k}_p^{(a)}(\boldsymbol{\kappa}) + k_z^{(a)}(\boldsymbol{\kappa})\mathbf{z}^{(a)}(0), \quad (9)$$

where $\mathbf{k}_p^{(a)}(\boldsymbol{\kappa})$ is a 2D planar vector lying in the plane perpendicular to $\mathbf{z}^{(a)}(0)$; it is

$$\mathbf{k}_p^{(a)}(\boldsymbol{\kappa}) = k_x^{(a)}(\boldsymbol{\kappa})\mathbf{x}^{(a)}(0) + k_y^{(a)}(\boldsymbol{\kappa})\hat{\mathbf{y}}. \quad (10)$$

Let us take the components of the vector $\mathbf{k}_p^{(i)}(\boldsymbol{\kappa})$ as the variables; i.e., let us assume that

$$\kappa_x \equiv k_x^{(i)}, \quad \kappa_y \equiv k_y^{(i)}. \quad (11)$$

It is evident that

$$k_y^{(\rho)}(\boldsymbol{\kappa}) = k_y^{(\tau)}(\boldsymbol{\kappa}) = \kappa_y. \quad (12)$$

As for the components $k_x^{(\rho)}(\boldsymbol{\kappa})$ and $k_x^{(\tau)}(\boldsymbol{\kappa})$, their dependence on κ_x and κ_y will be discussed below.

The amplitudes of the plane waves in the a th beam. Every vector $\mathcal{E}^{(a)}(\boldsymbol{\kappa})$ is orthogonal to the vector $\mathbf{k}^{(a)}(\boldsymbol{\kappa})$, so,

$$\mathcal{E}^{(a)}(\boldsymbol{\kappa}) = \mathcal{E}_x^{(a)}(\boldsymbol{\kappa})\mathbf{x}^{(a)}(\boldsymbol{\kappa}) + \mathcal{E}_y^{(a)}(\boldsymbol{\kappa})\hat{\mathbf{y}}(\boldsymbol{\kappa}). \quad (13)$$

The components of the vectors $\mathcal{E}^{(\rho)}(\boldsymbol{\kappa})$ and $\mathcal{E}^{(\tau)}(\boldsymbol{\kappa})$ are related to the respective components of the vector $\mathcal{E}^{(i)}(\boldsymbol{\kappa})$ by means of the Fresnel laws; they can be written as follows:

$$\mathcal{E}_x^{(\alpha)}(\boldsymbol{\kappa}) = q_x^{(\alpha)}(\boldsymbol{\kappa})\mathcal{E}_x^{(i)}(\boldsymbol{\kappa}), \quad \mathcal{E}_y^{(\alpha)}(\boldsymbol{\kappa}) = q_y^{(\alpha)}(\boldsymbol{\kappa})\mathcal{E}_y^{(i)}(\boldsymbol{\kappa}), \quad (14)$$

where $q_y^{(\rho)}(\boldsymbol{\kappa})$ [$q_y^{(\tau)}(\boldsymbol{\kappa})$] and $q_x^{(\rho)}(\boldsymbol{\kappa})$ [$q_x^{(\tau)}(\boldsymbol{\kappa})$] are the well-known field reflection (refraction) coefficients of the $\hat{\mathbf{x}}^{(i)}(\boldsymbol{\kappa})$ - or $\hat{\mathbf{y}}(\boldsymbol{\kappa})$ -polarized plane wave with the wave vector $\mathbf{k}^{(i)}(\boldsymbol{\kappa})$; see, e.g., [1].

The refraction coefficients are

$$q_y^{(\tau)}(\boldsymbol{\kappa}) = \frac{2 \cos[\theta^{(i)}(\boldsymbol{\kappa})]}{\cos[\theta^{(i)}(\boldsymbol{\kappa})] + \sqrt{n^2 - \sin^2[\theta^{(i)}(\boldsymbol{\kappa})]}} \quad (15)$$

and

$$q_x^{(\tau)}(\boldsymbol{\kappa}) = \frac{2n \cos[\theta^{(i)}(\boldsymbol{\kappa})]}{n^2 \cos[\theta^{(i)}(\boldsymbol{\kappa})] + \sqrt{n^2 - \sin^2[\theta^{(i)}(\boldsymbol{\kappa})]}}, \quad (16)$$

where $n = n^{(2)}/n^{(1)}$, and $\theta^{(i)}(\boldsymbol{\kappa})$ is the angle of incidence of the plane wave with the wave vector $\mathbf{k}^{(i)}(\boldsymbol{\kappa})$, $\theta^{(i)}(\boldsymbol{\kappa}) = -\arccos[\hat{\mathbf{x}} \cdot \hat{\mathbf{z}}^{(i)}(\boldsymbol{\kappa})]$. The reflection coefficients $q_y^{(\rho)}(\boldsymbol{\kappa})$ and $q_x^{(\rho)}(\boldsymbol{\kappa})$ are related to $q_y^{(\tau)}(\boldsymbol{\kappa})$ and $q_x^{(\tau)}(\boldsymbol{\kappa})$ by

$$q_y^{(\rho)}(\boldsymbol{\kappa}) = q_y^{(\tau)}(\boldsymbol{\kappa}) - 1 \quad (17)$$

and

$$q_x^{(\rho)}(\boldsymbol{\kappa}) = nq_x^{(\tau)}(\boldsymbol{\kappa}) - 1. \quad (18)$$

The polarization of every plane wave in the incident beam will be characterized by a complex parameter

$$m(\boldsymbol{\kappa}) = \frac{\mathcal{E}_y^{(i)}(\boldsymbol{\kappa})}{\mathcal{E}_x^{(i)}(\boldsymbol{\kappa})}. \quad (19)$$

By the use of Eq. (19) as well as of Eqs. (13) and (14), the vector $\mathcal{E}^{(a)}(\boldsymbol{\kappa})$ can be written as follows:

$$\mathcal{E}^{(a)}(\boldsymbol{\kappa}) = Cf(\boldsymbol{\kappa})q^{(a)}(\boldsymbol{\kappa})\mathbf{e}^{(a)}(\boldsymbol{\kappa}). \quad (20)$$

Here $f(\boldsymbol{\kappa})$ is a dimensionless function, which represents a form factor of the incident beam; we suppose that

$$\int |f(\boldsymbol{\kappa})|^2 d^2\boldsymbol{\kappa} = 1, \quad (21)$$

C is the normalization factor of this beam,

$$\mathbf{e}^{(a)}(\boldsymbol{\kappa}) = \frac{q_x^{(a)}(\boldsymbol{\kappa})\mathbf{x}^{(a)}(\boldsymbol{\kappa}) + q_y^{(a)}(\boldsymbol{\kappa})m(\boldsymbol{\kappa})\hat{\mathbf{y}}(\boldsymbol{\kappa})}{\sqrt{|q_x^{(a)}(\boldsymbol{\kappa})|^2 + |q_y^{(a)}(\boldsymbol{\kappa})m(\boldsymbol{\kappa})|^2}}, \quad (22)$$

and

$$q^{(a)}(\boldsymbol{\kappa}) = \sqrt{\frac{|q_x^{(a)}(\boldsymbol{\kappa})|^2 + |q_y^{(a)}(\boldsymbol{\kappa})m(\boldsymbol{\kappa})|^2}{|1 + m(\boldsymbol{\kappa})|^2}}. \quad (23)$$

It is assumed in Eqs. (20), (22), and (23) that $q_x^{(i)}(\boldsymbol{\kappa}) = q_y^{(i)}(\boldsymbol{\kappa}) = 1$; as a consequence, $q^{(i)}(\boldsymbol{\kappa}) = 1$ as well. Under such an assumption, these equations represent the vectors $\mathcal{E}^{(\rho)}(\boldsymbol{\kappa})$ and $\mathcal{E}^{(\tau)}(\boldsymbol{\kappa})$ as well as the vector $\mathcal{E}^{(i)}(\boldsymbol{\kappa})$. $\mathbf{e}^{(i)}(\boldsymbol{\kappa})$ and $\mathbf{e}^{(\rho)}(\boldsymbol{\kappa})$, as well as $\mathbf{e}^{(\tau)}(\boldsymbol{\kappa})$ in the partial-reflection regime, are the unit vectors. $[\mathbf{e}^{(a)}(\boldsymbol{\kappa})]^2 = 1$.

Further on, the characteristics of the central plane wave will be written without the argument 0. In particular, the

following denotations will be used: $m \equiv m(0)$, $q_x^{(a)} \equiv q_x^{(a)}(0)$, $q_y^{(a)} \equiv q_y^{(a)}(0)$, $\mathbf{e}^{(a)} \equiv \mathbf{e}^{(a)}(0)$, and $\mathcal{E}^{(a)} \equiv \mathcal{E}^{(a)}(0)$.

In the special case of well-defined IOAM of the incident beam,

$$f(\boldsymbol{\kappa}) = \phi(\kappa) \exp(-il\varphi), \quad (24)$$

where φ is the azimuth in the frame attached to the incident beam, $\varphi = \arctan(\kappa_y/\kappa_x)$, and l is the azimuthal index, $l = 0, \pm 1, \pm 2, \pm 3, \dots$. In this case the amplitude $\phi(\kappa)$ is independent of φ .

The vector $\mathcal{H}^{(a)}(\boldsymbol{\kappa})$ is related to the vector $\mathcal{E}^{(a)}(\boldsymbol{\kappa})$ by

$$\mathcal{H}^{(a)}(\boldsymbol{\kappa}) = n^{(a)} \mathbf{z}^{(a)}(\boldsymbol{\kappa}) \times \mathcal{E}^{(a)}(\boldsymbol{\kappa}). \quad (25)$$

The global electromagnetic field. Let us denote the electric and magnetic vectors of the global field by the letters $\mathbf{E}(\mathbf{r})$ and $\mathbf{H}(\mathbf{r})$ without the superscripts:

$$\mathbf{E}(\mathbf{r}) = \mathbf{E}^{(1)}(\mathbf{r}) + \mathbf{E}^{(2)}(\mathbf{r}), \quad \mathbf{H}(\mathbf{r}) = \mathbf{H}^{(1)}(\mathbf{r}) + \mathbf{H}^{(2)}(\mathbf{r}), \quad (26)$$

where $\mathbf{E}^{(1)}(\mathbf{r})[\mathbf{H}^{(1)}(\mathbf{r})]$ and $\mathbf{E}^{(2)}(\mathbf{r})[\mathbf{H}^{(2)}(\mathbf{r})]$ are the electric (magnetic) field vectors in the first and the second medium, respectively. It is evident that

$$\mathbf{E}^{(2)}(\mathbf{r}) = \mathbf{E}^{(\tau)}(\mathbf{r}), \quad \mathbf{H}^{(2)}(\mathbf{r}) = \mathbf{H}^{(\tau)}(\mathbf{r}), \quad (27)$$

while

$$\mathbf{E}^{(1)}(\mathbf{r}) = \mathbf{E}^{(i)}(\mathbf{r}) + \mathbf{E}^{(\rho)}(\mathbf{r}), \quad \mathbf{H}^{(1)}(\mathbf{r}) = \mathbf{H}^{(i)}(\mathbf{r}) + \mathbf{H}^{(\rho)}(\mathbf{r}). \quad (28)$$

The average rates of changes of the functions $f(\boldsymbol{\kappa})$, $k_x^{(a)}(\boldsymbol{\kappa})$, $q_x^{(a)}(\boldsymbol{\kappa})$, $q_y^{(a)}(\boldsymbol{\kappa})$, and $m(\boldsymbol{\kappa})$. Let us denote by b the characteristic dimension of the incident beam in the plane perpendicular to its axis [21]. As the beam is assumed to be paraxial, then

$$b \gg \Lambda. \quad (29)$$

Next, let us denote by $\Delta\kappa_x$ and $\Delta\kappa_y$ the intervals of κ_x and κ_y , where $|f(\boldsymbol{\kappa})|$ significantly differs from zero. As the characteristic dimension of the incident beam is b , then

$$\Delta\kappa_x \sim b^{-1}, \quad \Delta\kappa_y \sim b^{-1}. \quad (30)$$

Consider the average rates of changes of the functions $k_x^{(a)}(\boldsymbol{\kappa})$, $q_x^{(a)}(\boldsymbol{\kappa})$, $q_y^{(a)}(\boldsymbol{\kappa})$, and $m(\boldsymbol{\kappa})$ in the intervals $\Delta\kappa_x$ and $\Delta\kappa_y$. Using Snell's law, $k_x^{(a)}(\boldsymbol{\kappa})$ can be written as follows:

$$k_x^{(a)}(\boldsymbol{\kappa}) = \kappa_x(\zeta^{(a)} + \delta_{a\tau} O(\Lambda|\kappa|)), \quad (31)$$

where

$$\zeta^{(i)} = 1, \quad \zeta^{(\rho)} = -1, \quad \zeta^{(\tau)} = \frac{\cos \theta^{(i)}}{\cos \theta^{(\tau)}}, \quad (32)$$

and $\delta_{aa'}$ is the Kronecker delta.

The average rates of change of the functions $q_x^{(a)}(\boldsymbol{\kappa})$ and $q_y^{(a)}(\boldsymbol{\kappa})$ can be defined on the basis of Eqs. (15)–(18). It follows from these equations that in the regular region of $\theta^{(i)}$ [22],

$$\Delta\kappa_x \left| \frac{dq_x^{(a)}(\boldsymbol{\kappa})}{d\kappa_x} \right|_{\boldsymbol{\kappa}=0} = O\left(\frac{\Lambda}{b}\right) \quad (33)$$

and

$$\Delta\kappa_x \left| \frac{dq_y^{(a)}(\boldsymbol{\kappa})}{d\kappa_x} \right|_{\boldsymbol{\kappa}=0} = O\left(\frac{\Lambda}{b}\right), \quad (34)$$

see, e.g., Eqs. (17), (18), and (20) in [23], while the average rates of change of these functions in the interval $\Delta\kappa_y$ are much smaller.

Let us proceed to the parameter $m(\boldsymbol{\kappa})$. Its rate of change, like that of $q_x^{(a)}(\boldsymbol{\kappa})$ and $q_y^{(a)}(\boldsymbol{\kappa})$, can be characterized by the first derivatives. Let us use the following denotation:

$$\eta_x = \left| \frac{dm(\boldsymbol{\kappa})}{d\kappa_x} \right|_{\boldsymbol{\kappa}=0}, \quad \eta_y = \left| \frac{dm(\boldsymbol{\kappa})}{d\kappa_y} \right|_{\boldsymbol{\kappa}=0}. \quad (35)$$

As the incident beam is paraxial, then η_x and η_y must be small in comparison with b . However, this requirement can be specified, because in the actual cases the scale of η_x and η_y is Λ . For instance, it is known that if the polarization of the incident beam is constant across its cross section, then

$$\eta_x \Delta\kappa_x = O\left(\frac{\Lambda}{b}\right), \quad \eta_y \Delta\kappa_y = O\left(\frac{\Lambda}{b}\right); \quad (36)$$

see, e.g., [24,25]. In view of this, we will assume for the sake of simplicity that for every incident beam under consideration, the average rate of change of the function $m(\boldsymbol{\kappa})$ is similar to that of the function $q_x^{(a)}(\boldsymbol{\kappa})$ or $q_y^{(a)}(\boldsymbol{\kappa})$, i.e., that the conditions (36) are satisfied.

IV. THE DENSITIES OF THE LINEAR AND ANGULAR MOMENTA

The local densities of LMs. In the main part of the body of the paper and in every Appendix we will assume that LM is defined in the sense of Abraham. In this case the local density of the global LM

$$\mathbf{g}(\mathbf{r}) = \frac{1}{8\pi} \text{Re}[\mathbf{E}(\mathbf{r}) \times \mathbf{H}^*(\mathbf{r})], \quad (37)$$

where Re denotes the real part of an expression, and the asterisk denotes complex conjugation. The vector $\mathbf{g}(\mathbf{r})$ is assumed to be circle-averaged,

$$\mathbf{g}(\mathbf{r}) = \mathbf{g}^{(1)}(\mathbf{r}) + \mathbf{g}^{(2)}(\mathbf{r}), \quad (38)$$

where $\mathbf{g}^{(1)}(\mathbf{r})$ and $\mathbf{g}^{(2)}(\mathbf{r})$ are the LM densities in the first and the second medium, respectively. It is evident that

$$\mathbf{g}^{(2)}(\mathbf{r}) = \mathbf{g}^{(\tau\tau)}(\mathbf{r}), \quad (39)$$

while

$$\mathbf{g}^{(1)}(\mathbf{r}) = \mathbf{g}^{(ii)}(\mathbf{r}) + \mathbf{g}^{(\rho\rho)}(\mathbf{r}) + \mathbf{g}^{(i\rho)}(\mathbf{r}). \quad (40)$$

Here $\mathbf{g}^{(aa)}(\mathbf{r})$ is the LM density in the a th beam,

$$\mathbf{g}^{(aa)}(\mathbf{r}) = \frac{1}{8\pi} \text{Re}[\mathbf{E}^{(a)}(\mathbf{r}) \times \mathbf{H}^{(a)*}(\mathbf{r})], \quad (41)$$

and $\mathbf{g}^{(i\rho)}(\mathbf{r})$ is the density of the interference LM in the first medium,

$$\mathbf{g}^{(i\rho)}(\mathbf{r}) = \frac{1}{8\pi} \text{Re}[\mathbf{E}^{(i)}(\mathbf{r}) \times \mathbf{H}^{(\rho)*}(\mathbf{r}) + \mathbf{E}^{(\rho)}(\mathbf{r}) \times \mathbf{H}^{(i)*}(\mathbf{r})]. \quad (42)$$

Let us substitute Eqs. (3), (4) into Eqs. (41), (42) and use the relation (25). Then, after some vector algebra the vector $\mathbf{g}^{(aa')}(\mathbf{r})$ can be represented as the sum of two terms, see [26]:

$$\mathbf{g}^{(aa')}(\mathbf{r}) = \mathbf{g}_{\parallel}^{(aa')}(\mathbf{r}) + \mathbf{g}_{\perp}^{(aa')}(\mathbf{r}). \quad (43)$$

Every vector $\mathbf{g}_\beta^{(aa')}(\mathbf{r})$ ($\beta \in \{\parallel, \perp\}$) is

$$\mathbf{g}_\beta^{(aa')}(\mathbf{r}) = \frac{2 - \delta_{aa'}}{2^6 \pi^3} n^{(1)} \Lambda \text{Re} \iint \mathbf{u}_\beta^{(aa')}(\boldsymbol{\kappa}, \boldsymbol{\kappa}') \times \exp[i\mathbf{K}_-^{(aa')}(\boldsymbol{\kappa}, \boldsymbol{\kappa}') \cdot \mathbf{r}] d^2\boldsymbol{\kappa} d^2\boldsymbol{\kappa}', \quad (44)$$

where

$$\mathbf{u}_\parallel^{(aa')}(\boldsymbol{\kappa}, \boldsymbol{\kappa}') = \mathbf{K}_+^{(aa')}(\boldsymbol{\kappa}, \boldsymbol{\kappa}') [\mathcal{E}^{(a')}(\boldsymbol{\kappa}') \cdot \mathcal{E}^{(a)*}(\boldsymbol{\kappa})], \quad (45)$$

$$\mathbf{u}_\perp^{(aa')}(\boldsymbol{\kappa}, \boldsymbol{\kappa}') = \mathbf{K}_-^{(aa')}(\boldsymbol{\kappa}, \boldsymbol{\kappa}') \times \mathcal{E}^{(a')}(\boldsymbol{\kappa}') \times \mathcal{E}^{(a)*}(\boldsymbol{\kappa}), \quad (46)$$

and

$$\mathbf{K}_\pm^{(aa')}(\boldsymbol{\kappa}, \boldsymbol{\kappa}') = \mathbf{k}^{(a)*}(\boldsymbol{\kappa}) \pm \mathbf{k}^{(a')}(\boldsymbol{\kappa}'). \quad (47)$$

Note that the decomposition of the LM density or the Poynting vector similar to one given by Eqs. (43)–(47) was used in many previous works, where the rotation energy motion in the beams of homogeneous plane waves was considered (see, e.g., [27–32]); in application to the wave packet, a similar procedure has been realized in [14] [see Eqs. (15) and (15a) therein]. On the other hand, in the limiting case $f(\boldsymbol{\kappa}) \rightarrow \delta(\boldsymbol{\kappa})$, where $\delta(\boldsymbol{\kappa})$ is the 2D delta function, the above expression for $\mathbf{g}^{(\tau\tau)}(\mathbf{r})$ at total reflection coincides with the expression for the Poynting vector in the solitary inhomogeneous plane waves, which has been derived in [3,7].

The following distinction between the vectors $\mathbf{u}_\parallel^{(aa')}(\boldsymbol{\kappa}, \boldsymbol{\kappa}')$ and $\mathbf{u}_\perp^{(aa')}(\boldsymbol{\kappa}, \boldsymbol{\kappa}')$ should be mentioned: the former is parallel to the vector $\mathbf{K}_+^{(aa')}(\boldsymbol{\kappa}, \boldsymbol{\kappa}')$, while the latter is perpendicular to the vector $\mathbf{K}_-^{(aa')}(\boldsymbol{\kappa}, \boldsymbol{\kappa}')$. In particular, the y component of the vector $\mathbf{u}_\parallel^{(aa')}(\boldsymbol{\kappa}, \boldsymbol{\kappa}')$, which will be denoted as $u_{\parallel,y}^{(aa')}(\boldsymbol{\kappa}, \boldsymbol{\kappa}')$, is proportional to $(\kappa_y + \kappa'_y)$, while the y component of the vector $\mathbf{u}_\perp^{(aa')}(\boldsymbol{\kappa}, \boldsymbol{\kappa}')$ is proportional to the component of the vector $\mathbf{K}_-^{(aa')}(\boldsymbol{\kappa}, \boldsymbol{\kappa}')$, which is perpendicular to the y axis.

We will also divide LMs according to another criterion. LMs in the beams of homogeneous plane waves will be called LMs of the first class; LM in the inhomogeneous plane waves and the interference LM will be called LMs of the second class. The reason for such a division of LMs is elucidated in Sec. V and Appendix A. LMs of the first and the second classes will be marked by one dot and two dots over the respective letters. So, $\dot{\mathbf{g}}_\beta^{(aa)}(\mathbf{r})$ denotes $\mathbf{g}_\beta^{(ii)}(\mathbf{r})$ and $\mathbf{g}_\beta^{(\rho\rho)}(\mathbf{r})$ as well as $\mathbf{g}_\beta^{(\tau\tau)}(\mathbf{r})$ at $n^{(2)} > n^{(1)}$ or $n^{(2)} < n^{(1)}$ and $\theta^{(i)} < \theta^{(iC)}$, while $\ddot{\mathbf{g}}_\beta^{(aa')}(\mathbf{r})$ denotes $\mathbf{g}_\beta^{(\tau\tau)}(\mathbf{r})$ at $n^{(2)} < n^{(1)}$ and $\theta^{(i)} > \theta^{(iC)}$ and $\mathbf{g}_\beta^{(i\rho)}(\mathbf{r})$.

LM per unit length (*pul*) of the beam of homogeneous plane waves. Let us denote LM *pul* of the beam of homogeneous plane waves by $\dot{\mathbf{I}}^{(aa)}(z^{(a)})$. According to Eq. (43), $\dot{\mathbf{I}}^{(aa)}(z^{(a)}) = \dot{\mathbf{I}}_{\parallel,z}^{(aa)}(z^{(a)}) + \dot{\mathbf{I}}_{\perp}^{(aa)}(z^{(a)})$, and every

$$\dot{\mathbf{I}}_\beta^{(aa)}(z^{(a)}) = \int_{-\infty}^{\infty} dy \int_{\gamma_-^{(a)}}^{\gamma_+^{(a)}} dx^{(a)} \dot{\mathbf{g}}_\beta^{(aa)}(\mathbf{r}), \quad (48)$$

where

$$\gamma_+^{(i,\rho)} = -\gamma_-^{(\tau)} = \infty, \quad (49)$$

while

$$\gamma_-^{(i,\rho)} = z^{(i,\rho)} \cot \theta^{(i,\rho)}, \quad \gamma_+^{(\tau)} = z^{(\tau)} \cot \theta^{(\tau)}. \quad (50)$$

Let consider the beam's cross section that is situated far from the point O where the condition

$$|z^{(a)}| \gg b |\tan \theta^{(a)}| \quad (51)$$

is fulfilled. In this region of $z^{(a)}$ the finite limit of integration with respect to $x^{(a)}$ can be replaced by the infinite one; so, $\dot{\mathbf{I}}^{(aa)}(z^{(a)})$ approximately coincides there with LM *pul* of the beam whose field vectors are given by Eqs. (3) and (4) but which propagates in the homogeneous medium with the dielectric constant $\epsilon^{(a)}$. Let us substitute Eq. (45) or (46) into the right-hand side of Eq. (44) and the result into the right-hand side of Eq. (48). Then, let us carry out the integrations over $x^{(a)}$ and y , both from $-\infty$ to ∞ , and after that the integration with respect to $\boldsymbol{\kappa}'$. Let us also use the relations (20) and (21). We obtain that the vector $\dot{\mathbf{I}}^{(aa)}(z^{(a)})$ is approximately independent of $z^{(a)}$ in the region (51); when considered in the region (51), this vector will be written as $\dot{\mathbf{I}}^{(aa)}$ without the argument $z^{(a)}$. We also obtain that $\dot{\mathbf{I}}_{\perp}^{(aa)} = 0$, so

$$\dot{\mathbf{I}}^{(aa)} = \dot{\mathbf{I}}_{\parallel}^{(aa)}. \quad (52)$$

Bearing in mind the aim of this paper, only the axial and transverse components of the vector $\dot{\mathbf{I}}^{(aa)}$ will further be considered; they are $\dot{\Gamma}_{\parallel,z}^{(aa)} = \hat{\mathbf{z}}^{(a)} \cdot \dot{\mathbf{I}}_{\parallel,z}^{(aa)} = \hat{\mathbf{z}}^{(a)} \cdot \dot{\mathbf{I}}^{(aa)}$, and $\dot{\Gamma}_{\parallel,y}^{(aa)} = \hat{\mathbf{y}} \cdot \dot{\mathbf{I}}_{\parallel}^{(aa)} = \hat{\mathbf{y}} \cdot \dot{\mathbf{I}}^{(aa)}$.

$\dot{\Gamma}_{\parallel,z}^{(ii)}$ can be expressed through the normalization coefficient C . In the zero-order approximation, when the dependence of $m(\boldsymbol{\kappa})$ on $\boldsymbol{\kappa}$ is ignored,

$$\Gamma_{\parallel,z}^{(ii)} = \frac{n^{(1)}}{8\pi} |C|^2. \quad (53)$$

When the dependence of $q^{(a)}(\boldsymbol{\kappa})$ on $\boldsymbol{\kappa}$ is also ignored, then the expression for every $\dot{\Gamma}_{\parallel,z}^{(aa)}$ can be written as follows:

$$\dot{\Gamma}_{\parallel,z}^{(aa)} = Q^{(a)} \Gamma_{\parallel,z}^{(ii)}, \quad (54)$$

where

$$Q^{(a)} = \frac{n^{(a)}}{n^{(1)}} \frac{1}{|\zeta^{(a)}|} |q^{(a)}|^2. \quad (55)$$

$Q^{(\rho)}$ and $Q^{(\tau)}$ are the reflectivity and transmissivity for the incident plane wave with the wave vector $\mathbf{k}^{(i)}$, while $Q^{(i)} = 1$, because $q^{(i)} = 1$.

As for the transverse component of the vector $\dot{\mathbf{I}}_{\parallel}^{(aa)}$, it can be expressed in terms of $\dot{\Gamma}_{\parallel,z}^{(ii)}$ as follows:

$$\dot{\Gamma}_{\parallel,y}^{(aa)} = \Gamma_{\parallel,z}^{(ii)} \int \frac{\Lambda \kappa_y}{|\zeta^{(a)}(\boldsymbol{\kappa})|} |q^{(a)}(\boldsymbol{\kappa})|^2 |f(\boldsymbol{\kappa})|^2 d^2\boldsymbol{\kappa}, \quad (56)$$

where

$$\zeta^{(a)}(\boldsymbol{\kappa}) = \frac{dk_x^{(a)}(\boldsymbol{\kappa})}{d\kappa_x}. \quad (57)$$

$\Gamma_{\parallel,y}^{(ii)}$ as well as the $x^{(a)}$ component of the vector $\Gamma_{\parallel}^{(ii)}$ must be equal to zero. This requirement together with the choice of

the point O defines the frame attached to the incident beam. The condition

$$\Gamma_{\parallel,y}^{(ii)} = 0 \quad (58)$$

means that the incident beam's axis is parallel to the plane of incidence. Using Eq. (56) and taking into account that $\zeta^{(i)}(\boldsymbol{\kappa}) = 1$, $q^{(i)}(\boldsymbol{\kappa}) = 1$, one can conclude that this condition is equivalent to the following constraint on the function $f(\boldsymbol{\kappa})$:

$$\int \kappa_y |f(\boldsymbol{\kappa})|^2 d^2\boldsymbol{\kappa} = 0. \quad (59)$$

If the condition (59) is fulfilled, then at total reflection $\Gamma_{\parallel,y}^{(\rho\rho)} = 0$. In the partial-reflection regime $\Gamma_{\parallel,y}^{(\rho\rho)}$ and $\dot{\Gamma}_{\parallel,y}^{(\tau\tau)}$ can have nonzero values. If $\dot{\Gamma}_{\parallel,y}^{(\alpha\alpha)} \neq 0$, then the angular TShCG of the α th beam occurs [23,25,31,33–36]. In this case the actual axis of the secondary beam is inclined to the plane of incidence, the angle of inclination being approximately equal to $\dot{\Gamma}_{\parallel,y}^{(\alpha\alpha)}/\dot{\Gamma}_{\parallel,z}^{(\alpha\alpha)}$.

From the point of view of the TLM phenomenon, it is essential that nonzero value of $\dot{\Gamma}_{\parallel,y}^{(\alpha\alpha)}$ gives rise to the bulk TLM of the respective secondary beam, i.e., to TLM that is proportional to the length of the beam. The detailed analysis of this effect is not the aim of the present paper. Further on, the condition will be established when the bulk TLMs are small in comparison with STLMS; the establishment will be based on the estimation the scale of $\dot{\Gamma}_{\parallel,y}^{(\alpha\alpha)}$. The value of the dimensionless integral on the right-hand side of Eq. (56) can be estimated by the use of the relations (30), (31), (33), (34), (36), and (59). Taking into account these relations one can conclude that in the partial-reflection regime

$$\frac{|\dot{\Gamma}_{\parallel,y}^{(\alpha\alpha)}|}{\dot{\Gamma}_{\parallel,z}^{(ii)}} = O\left(\frac{\Lambda^2}{b^2}\right). \quad (60)$$

This estimation is in agreement with the results of calculations of the specific angular TShCGs of secondary beams [23,25,33].

The spin and IOAM of the beam of homogeneous plane waves. Further on, we will analyze the relationships between IOAMs and STLMS of the beams as well as the relationships between the spins and STLMS. In view of that, IAM *pul* of the a th beam of homogeneous plane waves will later be considered; it will be denoted by $\dot{\mathbf{I}}^{(aa)}(z^{(a)})$. Like previously, here we assume that the $z^{(a)}$ coordinate of the a th beam is restricted by the condition (51); in this region of $z^{(a)}$ the vector $\dot{\mathbf{I}}^{(aa)}$, like the vector $\dot{\Gamma}^{(aa)}$, is approximately independent of $z^{(a)}$ and is directed along the axis of the a th beam, i.e., $\dot{\mathbf{I}}^{(aa)} = \dot{j}^{(aa)}\hat{\mathbf{z}}^{(a)}$.

$\dot{j}^{(aa)}$, like $\mathbf{g}^{(aa')}(\mathbf{r})$ and $\mathbf{\Gamma}^{(aa)}$, is the sum of two terms,

$$\dot{j}^{(aa)} = \dot{j}_{\parallel}^{(aa)} + \dot{j}_{\perp}^{(aa)}. \quad (61)$$

Every term $\dot{j}_{\beta}^{(aa)}$, in turn, is also the sum of two terms,

$$\dot{j}_{\beta}^{(aa)} = \dot{j}_{\beta,[yx]}^{(aa)} + \dot{j}_{\beta,[xy]}^{(aa)}, \quad (62)$$

where $\dot{j}_{\beta,[yx]}^{(aa)}$ is defined as follows:

$$\dot{j}_{\beta,[yx]}^{(aa)} = \int_{-\infty}^{\infty} dx^{(a)} \int_{-\infty}^{\infty} dy x^{(a)} g_{\beta,y}^{(aa)}(\mathbf{r}), \quad (63)$$

while $\dot{j}_{\beta,[xy]}^{(aa)}$ is given by the right-hand side of Eq. (63) provided that $x^{(a)}$ in the integrand is replaced by $-y$ and $g_{\beta,y}^{(aa)}$ by $g_{\beta,x}^{(aa)}$.

We begin with calculating $\dot{j}_{\parallel}^{(aa)}$ and first consider its part $\dot{j}_{\parallel,[yx]}^{(aa)}$. Let us substitute Eq. (45) into the right-hand side of Eq. (44) and the result into the right-hand side of Eq. (63). Next, let us take into account that $k_x^{(\tau)}(\boldsymbol{\kappa}) \cong \zeta^{(\tau)}\kappa_x$ and that $x^{(a)} \exp(-i\zeta^{(a)}\kappa_x'x^{(a)}) = i(1/\zeta^{(a)})d/d\kappa_x' \exp(-i\zeta^{(a)}\kappa_x'x^{(a)})$. Then, the integration by parts over κ_x' and after that the integrations over the other variables leads to

$$\dot{j}_{\parallel,[yx]}^{(aa)} = \frac{n^{(1)}}{n^{(a)}} \mathcal{Q}^{(a)} L_{[yx]}^{(aa)} \Upsilon. \quad (64)$$

Here

$$\Upsilon = \Lambda \Gamma_{\parallel,z}^{(ii)}, \quad (65)$$

this factor defines the scale of $\dot{j}_{\parallel,[yx]}^{(aa)}$. The other factors on the right-hand side of Eq. (64) are dimensionless,

$$L_{[yx]}^{(ii)} = -i \int f^*(\boldsymbol{\kappa}) \kappa_y \frac{d}{d\kappa_x} f(\boldsymbol{\kappa}) d^2\boldsymbol{\kappa}, \quad (66)$$

while $L_{[yx]}^{(\alpha\alpha)}$ is related to $L_{[yx]}^{(ii)}$ by

$$L_{[yx]}^{(\alpha\alpha)} = \frac{1}{\zeta^{(a)}} L_{[yx]}^{(ii)}. \quad (67)$$

$\dot{j}_{\parallel,[xy]}^{(aa)}$ is given by Eqs. (64)–(67) provided that the following replacements are made: $L_{[yx]}^{(aa)} \rightarrow L_{[xy]}^{(aa)}$ in Eqs. (64), (66), and (67); $\kappa_y \rightarrow -\kappa_x$ and $d/d\kappa_x \rightarrow d/d\kappa_y$ in Eq. (66); and $1/\zeta^{(a)} \rightarrow \zeta^{(a)}$ in Eq. (67).

Note that the quantities $L_{[yx]}^{(aa)}$ and $L_{[xy]}^{(aa)}$ are not always equal. The equality takes place when IOAM of the a th beam is well defined, e.g., when the beam is the Laguerre-Gaussian one. It should be mentioned that IOAMs of all three beams considered cannot be well defined simultaneously. For instance, if IOAM of the incident beam is well defined, i.e., if the function $f(\boldsymbol{\kappa})$ is given by Eq. (24), and $L_{[yx]}^{(ii)} = L_{[xy]}^{(ii)} = 1/2$, then IOAM of the reflected beam is also well defined, as $\zeta^{(\rho)} = -1$; therefore, $L_{[xy]}^{(\rho\rho)} = L_{[yx]}^{(\rho\rho)} = -1/2$. On the other hand, $L_{[yx]}^{(\tau\tau)} \neq L_{[xy]}^{(\tau\tau)}$, as $\zeta^{(\tau)}$, unlike $|\zeta^{(\rho)}|$, is not an integer in the general case.

The way of calculating $\dot{j}_{\perp}^{(aa)}$ is similar to the way of calculating $\dot{j}_{\parallel}^{(aa)}$, but Eq. (46) instead of Eq. (45) should be substituted into the right-hand side of Eq. (44). Let us use the identity

$$\mathbf{K}_{-}^{(aa')} \exp(i\mathbf{K}_{-}^{(aa')} \cdot \mathbf{r}) = -i \frac{d}{d\mathbf{r}} \exp(i\mathbf{K}_{-}^{(aa')} \cdot \mathbf{r}) \quad (68)$$

and carry out the integration by parts over $x^{(a)}$ or y when calculating $\dot{j}_{\perp,[yx]}^{(aa)}$ or $\dot{j}_{\perp,[xy]}^{(aa)}$, respectively. The integrations with respect to the other variables are straightforward. If the aforementioned integrations have been carried out, we get

$$\dot{j}_{\perp,[yx]}^{(aa)} = \dot{j}_{\perp,[xy]}^{(aa)} = \frac{n^{(1)}}{n^{(a)}} \mathcal{Q}^{(a)} \frac{v^{(a)}}{2} \Upsilon, \quad (69)$$

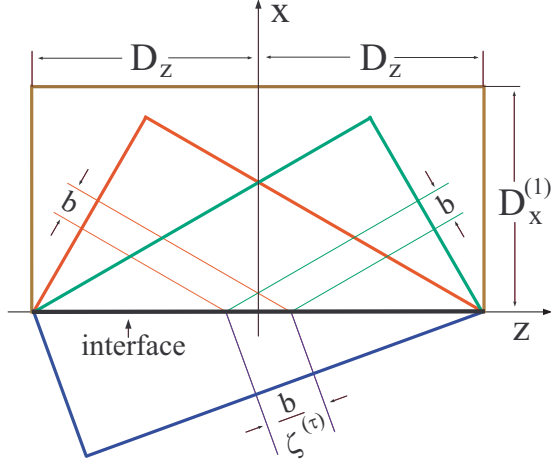


FIG. 2. The bases of the prisms $\dot{\mathcal{P}}^{(aa)}$ and $\mathcal{P}^{(i\rho)}$, $\mathcal{P}^{(ii)}$, the thick red lines; $\mathcal{P}^{(\rho\rho)}$, the thick green lines; $\dot{\mathcal{P}}^{(\tau\tau)}$, the thick blue lines; $\mathcal{P}^{(i\rho)}$, the thick brown lines. The thin colored lines mark the symbolic borders of the respective beams. The thick black line is the side of the basis of every prism adjusted to the interface. $n^{(2)} > n^{(1)}$.

where

$$v^{(a)} = -i\hat{\mathbf{z}}^{(a)} \cdot \hat{\mathbf{e}}^{(a)} \times \hat{\mathbf{e}}^{(a)*} = \frac{2\text{Im}[q_x^{(a)}(q_y^{(a)}m)^*]}{|q_x^{(a)}|^2 + |q_y^{(a)}m|^2}; \quad (70)$$

the sign Im denotes the imaginary part of an expression. Note that the right-hand sides of the relations (64) and (69) are similar.

V. THE CALCULATIONS OF STLMS

The ways of calculating particular STLMS. Let us consider the (aa') th TLM confined in a domain adjacent to the interface and assume that the domain is the same for $\beta \parallel$ and $\beta \perp$. The volume of the (aa') th domain will be denoted by $\mathcal{V}^{(aa')}$, and TLM confined in it by $G_{\beta,y}^{(aa')}(\mathcal{V}^{(aa')})$,

$$G_{\beta,y}^{(aa')}(\mathcal{V}^{(aa')}) = \int_{\mathcal{V}^{(aa')}} g_{\beta,y}^{(aa')}(\mathbf{r}) d^3\mathbf{r}. \quad (71)$$

Let every $\mathcal{V}^{(aa')}$ be the volume of a right prism whose base faces are parallel to the plane of incidence, their y coordinates being equal to $\pm D_y$. Next, let the bases of the prisms, which will be used in order to calculate TLMs of the first and the second classes, be triangles and rectangles, respectively. Such prisms will be denoted by $\dot{\mathcal{P}}^{(aa)}$ and $\ddot{\mathcal{P}}^{(aa')}$ and their volumes by $\dot{\mathcal{V}}^{(aa)}$ and $\ddot{\mathcal{V}}^{(aa')}$. The bases of $\dot{\mathcal{P}}^{(aa)}$ and $\mathcal{P}^{(i\rho)}$ are depicted in Fig. 2; this figure is applied to the partial-reflection regime. One side of every triangle or rectangle is the segment $(-D_z, D_z)$ of a line, adjusted to the z axis. Two other sides of the (aa) th triangle are parallel and perpendicular to the $z^{(a)}$ axis; their lengths are evidently equal to $2D_z \sin \theta^{(a)}$ and $2D_z |\cos \theta^{(a)}|$, respectively. $D_x^{(1)}$ is the length of every side of the base of $\mathcal{P}^{(i\rho)}$ that is parallel to the x axis.

In the case of the total reflection, the shapes of the bases of $\mathcal{P}^{(ii)}$, $\mathcal{P}^{(\rho\rho)}$, and $\mathcal{P}^{(i\rho)}$ are the same as in the previous case. On the other hand, the base of $\ddot{\mathcal{P}}^{(\tau\tau)}$, unlike of $\dot{\mathcal{P}}^{(\tau\tau)}$, is the rectangle with the shape similar to the shape of the base of

$\mathcal{P}^{(i\rho)}$, but it is situated in the lower half plane. The length of the side of this rectangle that is parallel to the x axis will be denoted as $D_x^{(2)}$.

Let us assume that

$$D_y \gg b, \quad D_z \gg b, \quad D_x^{(1)} \gg b, \quad D_x^{(2)} \gg \Lambda, \quad (72)$$

and that $\theta^{(i)}$ is not close to 0 or $\pi/2$ and, when $n^{(2)} < n^{(1)}$, to $\theta^{(iC)}$.

Generally speaking, $G_{\beta,y}^{(aa')}(\mathcal{V}^{(aa')})$ can be separated into two parts that are independent of and dependent on the value of $\mathcal{V}^{(aa')}$; the former and the latter parts describe STLM and the bulk TLM, respectively. The present paper is devoted to investigation of STLMS; this part of the (aa') th TLM will be denoted as $G_{\beta,y}^{(aa')}$ without the argument $\mathcal{V}^{(aa')}$. It will later be shown that the bulk TLMs of the first class can be ignored if the following constraint on every $z^{(a)}$ is imposed:

$$|z^{(a)}| \ll b^2/\Lambda. \quad (73)$$

Therefore, we will consider only the near-field regions of the beams of homogeneous plane waves, where the condition (73) is fulfilled. According to this condition, the following constraint should be imposed on D_z :

$$D_z \ll \frac{b^2}{\sin(\theta^{(a)})\Lambda}. \quad (74)$$

Note that this relation is compatible with the second inequality in (72). As for the particular TLMs of the second class, their values are independent of the dimensions of $\mathcal{P}^{(i\rho)}$ and $\dot{\mathcal{P}}^{(\tau\tau)}$ if the conditions (72) are fulfilled.

The particular spin-dependent STLMS. We begin with calculating the particular TLMs $G_{\perp,y}^{(aa')}(\mathcal{V}^{(aa')})$. Let us substitute Eq. (46) into the right-hand side of Eq. (44) and then Eq. (44) into the right-hand side of Eq. (71). Let us also use the identity (68). By means of this identity and the rotor theorem, the integral of $g_{\perp,y}^{(aa')}(\mathbf{r})$ over the volume $\dot{\mathcal{V}}^{(aa)}$ or $\ddot{\mathcal{V}}^{(aa')}$ can be converted into the sum of the surface integrals over N sides of the respective prism: five sides of $\dot{\mathcal{P}}^{(aa)}$ or six sides of $\ddot{\mathcal{P}}^{(aa')}$. Then carrying out the integrations with respect to κ and κ' and taking into account Eq. (3), we get

$$G_{\perp,y}^{(aa')}(\mathcal{V}^{(aa')}) = \sum_N \int \hat{\mathbf{y}} \cdot \hat{\mathbf{N}}^{(aa')} \times \boldsymbol{\mu}^{(aa')}(\mathbf{r}_N^{(aa')}) d^2\mathbf{r}_N^{(aa')}, \quad (75)$$

where $\mathbf{r}_N^{(aa')}$ is a 2D vector lying on the N th side of the prism $\mathcal{P}^{(aa')}$, $\hat{\mathbf{N}}^{(aa')}$ is the unit outer-pointing normal to this side, and

$$\boldsymbol{\mu}^{(aa')}(\mathbf{r}) = \frac{2 - \delta_{aa'}}{16\pi} n^{(1)} \Lambda \text{Im}[\mathbf{E}^{(a)}(\mathbf{r}) \times \mathbf{E}^{(a')*}(\mathbf{r})]. \quad (76)$$

Let us first consider the particular spin-dependent TLMs of the second class. In this case 2D integrals over all sides of the prism $\mathcal{P}^{(i\rho)}$ or $\dot{\mathcal{P}}^{(\tau\tau)}$ except for one adjacent to the interface can be ignored. This is because the amplitudes of inhomogeneous waves at the aforementioned sides of $\dot{\mathcal{P}}^{(\tau\tau)}$ as well as the field of at least one beam, incident or reflected, at the respective sides of $\mathcal{P}^{(i\rho)}$ are negligible, if the conditions (72) are fulfilled [37]. For the same reason, when calculating the particular spin-dependent TLM of the first class, the surface integrals over all sides of the prism $\dot{\mathcal{P}}^{(aa)}$, except the sides adjacent to the interface and situated in the

beam's cross section, can be ignored. However, the latter can also be ignored, at least in the zero-order approximation. This is because $\hat{\mathbf{N}}^{(aa)} = \mp \hat{\mathbf{z}}^{(a)}$ on this side, while the vector $\mathbf{e}^{(a)} \times \mathbf{e}^{(a)*}$ is also parallel to the vector $\hat{\mathbf{z}}^{(a)}$. Hence, we get that every

$$G_{\perp,y}^{(aa')} (V^{(aa')}) = \pm \int_{-D_y}^{D_y} dy \int_{-D_z}^{D_z} dz \hat{\mathbf{z}} \cdot \boldsymbol{\mu}^{(aa')}(\pm \varepsilon, y, z). \quad (77)$$

Here and in Eqs. (78) and (82) the signs “+” and “−” stand for $aa' \in \{ii, \rho\rho, i\rho\}$ and $aa' \in \tau\tau$, respectively; $\varepsilon \rightarrow 0^+$.

Let us substitute Eq. (76) into the right-hand side of Eq. (77) and use the expression (3). Due to the conditions (72), the limits of integration over y and z can be replaced by $\pm\infty$. Then, carrying out these integrations, we get that every $G_{\perp,y}^{(aa')}(\mathcal{V}^{(aa')})$ is independent of the dimensions of $\mathcal{V}^{(aa')}$; i.e., it has no bulk part. As for the surface part, it is as follows:

$$G_{\perp,y}^{(aa')} = \pm \tan \theta^{(i)} \frac{\text{Im}(m^* \Psi^{(aa')})}{1 + |m|^2} \Upsilon, \quad (78)$$

where

$$\Psi^{(aa)} = \frac{n^{(1)}}{n^{(a)}} q_x^{(a)} q_y^{(a)*} \quad (79)$$

and

$$\Psi^{(i\rho)} = q_x^{(\rho)} + q_y^{(\rho)*}. \quad (80)$$

The quantity Υ is given by Eq. (65). It defines the scale of STLM, like the scale of IAM *pul* of the incident beam; compare Eq. (78) with Eqs. (64) and (69). It is also worth mentioning that Υ is LM confined to the sector of the incident beam of Λ length.

$G_{\perp,y}^{(aa')}$ depends on the polarization of the incident beam through the parameter m ; therefore, it can be called the spin-dependent STLM. Equations (78)–(80) give the particular spin-dependent STLMs of both classes. Taking into account the expression (69) for $\hat{I}_{\perp,[yx]}^{(aa)}$ as well as the expressions (55) and (70) for $Q^{(a)}$ and $v^{(a)}$, the particular spin-dependent STLM of the first class can be represented as follows:

$$\hat{G}_{\perp,y}^{(aa)} \cong \pm \tan \theta^{(a)} \hat{I}_{\perp,[yx]}^{(aa)} \cong \pm \frac{1}{2} \tan \theta^{(a)} \hat{I}_{\perp}^{(aa)}. \quad (81)$$

Here the signs “+” and “−” stand for $a \in i$ and $a \in \alpha$, respectively. The expression (81) clearly indicates how $\hat{G}_{\perp,y}^{(aa)}$ is related to the spin of the a th beam.

Every $G_{\perp,y}^{(aa')}$ is independent of the space structure of the incident beam. In view of that, the relation (78) can be applied to the process of reflection and transmission of a plane electromagnetic wave. When a plane-wave approach is employed, it is more convenient to operate with PFs than with LMs. In order to turn to the plane-wave approach, let us denote the dimensions of the incident beam in the $x^{(i)}$ and y directions as $b_x^{(i)}$ and b_y . Next, let us assume that the incident beam is approximately homogeneous in the transverse direction. Then, dividing the left and right part of Eq. (78) by b_y and then making passages $b_y \rightarrow \infty$, $b_x^{(i)} \rightarrow \infty$, we get

$$P_{\perp,y}^{(aa')} = \pm \tan \theta^{(i)} \frac{\text{Im}(m^* \Psi^{(aa')})}{1 + |m|^2} P_z^{(ii)}, \quad (82)$$

where $P_{\perp,y}^{(aa')}$ is the (aa') th TPF through an infinite plane, and $P_z^{(ii)}$ is PF falling on the infinite strip in the cross section of the incident beam of Λ length in the transverse direction (compare with the results presented in Ref. [8]).

The particular IOAM-dependent STLMs. The way of calculating $G_{\parallel,y}^{(aa')}(\mathcal{V}^{(aa')})$ is different. Let us first consider these TLMs of the first class. When calculating $\hat{G}_{\parallel,y}^{(aa')}(\hat{\mathcal{V}}^{(aa')})$, it is convenient to use the coordinates $x^{(a)}$, y , and $z^{(a)}$. In this frame

$$\hat{G}_{\parallel,y}^{(aa')}(\hat{\mathcal{V}}^{(aa')}) = \int_{-D_z^{(a)}}^{D_z^{(a)}} dz^{(a)} \int_{-D_y}^{D_y} dy \int_{\hat{\gamma}_-^{(a)}}^{\hat{\gamma}_+^{(a)}} dx^{(a)} \hat{s}_{\parallel,y}^{(aa')}(\mathbf{r}), \quad (83)$$

where

$$D_z^{(a)} = D_z \sin \theta^{(a)}. \quad (84)$$

One limit of integration with respect to $x^{(a)}$ is proportional to $z^{(a)}$, namely, $\hat{\gamma}_-^{(i,\rho)} = \gamma_-^{(i,\rho)}$ and $\hat{\gamma}_+^{(\tau)} = \gamma_+^{(\tau)}$, where $\gamma_{\pm}^{(i,\rho)}$ is given by Eq. (50); the other limit is constant: $\hat{\gamma}_+^{(i,\rho)} = D_z |\cos \theta^{(i,\rho)}|$ and $\hat{\gamma}_-^{(\tau)} = -D_z \cos \theta^{(\tau)}$.

According to the conditions (72), both limits of integration with respect to y and one limit of integration with respect to $x^{(a)}$, $\hat{\gamma}_+^{(i,\rho)}$ or $\hat{\gamma}_-^{(\tau)}$, can be replaced by $\pm\infty$. In order to make such a replacement for the other limit of the latter integration, let us multiply the integrand in Eq. (83) by the Heaviside step function $\Theta(\pm v^{(a)})$, where $v^{(a)} = (x^{(a)} - z^{(a)} \cot \theta^{(a)})$; the signs “+” and “−” stand for $a \in \{i, \rho\}$ and $a \in \tau$, respectively. It is convenient to use the following integral representation of this function:

$$\Theta(\pm v^{(a)}) = \frac{i}{2\pi} \int_{-\infty}^{\infty} \frac{\exp(-i\tilde{\kappa} v^{(a)})}{\pm \tilde{\kappa} + i\varepsilon} d\tilde{\kappa}.$$

Let us subsequently substitute Eq. (45) into the right-hand side of Eq. (44) and the expression for $\hat{g}_{\parallel,y}^{(aa')}(\mathbf{r})$ obtained into the right-hand side of Eq. (83). Then, carrying out the integration over $x^{(a)}$ and y , both from $-\infty$ to $+\infty$, and after that the integration with respect to κ'_x , we get

$$\begin{aligned} \hat{G}_{\parallel,y}^{(aa')}(\hat{\mathcal{V}}^{(aa')}) &= -\frac{n^{(1)}\Lambda}{16\pi^2} \text{Im} \int_{-\infty}^{\infty} d\kappa_y \int_{-\infty}^{\infty} d\kappa_x \int_{-\infty}^{\infty} \frac{d\tilde{\kappa}}{\pm \tilde{\kappa} + i\varepsilon} \\ &\quad \times \int_{-D_z^{(a)}}^{D_z^{(a)}} dz^{(a)} \Omega(\boldsymbol{\kappa}, \tilde{\kappa}) \exp(i\tilde{\kappa} z^{(a)} \cot \theta^{(a)}), \end{aligned} \quad (85)$$

where

$$\Omega(\boldsymbol{\kappa}, \tilde{\kappa}) = \frac{\kappa_y \mathcal{E}^{(a)}(\kappa_x^a, \kappa_y) \cdot \mathcal{E}^{(a)*}(\kappa_x, \kappa_y)}{|\zeta^{(a)}(\kappa_x^a, \kappa_y)|}, \quad (86)$$

and where κ_x^a is a function of the variables κ_x , κ_y , and $\tilde{\kappa}$, it is defined by the equation $k_x^{(a)}(\kappa_x^a, \kappa_y) - k_x^{(a)}(\kappa_x, \kappa_y) + \tilde{\kappa} = 0$; note that $\kappa_x^a \rightarrow \kappa_x$ as $\tilde{\kappa} \rightarrow 0$. $\zeta^{(a)}(\kappa_x^a, \kappa_y)$ is given by Eq. (57).

Let us decompose $\hat{G}_{\parallel,y}^{(aa')}(\hat{\mathcal{V}}^{(aa')})$ into two parts as follows:

$$\hat{G}_{\parallel,y}^{(aa')}(\hat{\mathcal{V}}^{(aa')}) = \hat{G}_{\parallel,y}^{(aa,S)}(\hat{\mathcal{V}}^{(aa')}) + \hat{G}_{\parallel,y}^{(aa,B)}(\hat{\mathcal{V}}^{(aa')}), \quad (87)$$

where $\hat{G}_{\parallel,y}^{(aa,S)}(\hat{\mathcal{V}}^{(aa')})$ and $\hat{G}_{\parallel,y}^{(aa,B)}(\hat{\mathcal{V}}^{(aa')})$ are given by the right-hand side of Eq. (85), if the factor $\Omega(\boldsymbol{\kappa}, \tilde{\kappa})$ in the integrand is replaced by the factors $\Omega(\boldsymbol{\kappa}, \tilde{\kappa}) - \Omega(\boldsymbol{\kappa}, 0)$ and $\Omega(\boldsymbol{\kappa}, 0)$, respectively.

Let us first consider the term $\dot{G}_{\parallel,y}^{(aa,S)}(\dot{\mathcal{V}}^{(aa)})$. Note that once the aforementioned replacement in Eq. (85) is done, then the integrand does not contain a singularity, because $\Omega(\boldsymbol{\kappa}, \tilde{\kappa}) - \Omega(\boldsymbol{\kappa}, 0) \rightarrow 0$ as $\tilde{\kappa} \rightarrow 0$. Bearing in mind this fact as well as Eq. (84) and the second relation (72), the passage $D_z^{(a)} \rightarrow \infty$ can be made when calculating $\dot{G}_{\parallel,y}^{(aa,S)}(\dot{\mathcal{V}}^{(aa)})$. When such a passage is made, let us first carry out the integration over $z^{(a)}$ from $-\infty$ to ∞ and after that the integration with respect to $\tilde{\kappa}$. Next, let us take into account Eqs. (20)–(23) and (53)–(55). Then we get that $\dot{G}_{\parallel,y}^{(aa,S)}(\dot{\mathcal{V}}^{(aa)})$ is approximately independent of $\dot{\mathcal{V}}^{(aa)}$, so, it represents the (aa) th IOAM-dependent STLM. In the nearest-order approximation, when the dependence of the quantities $m(\boldsymbol{\kappa})$ and $q^{(\alpha)}(\boldsymbol{\kappa})$ on $\boldsymbol{\kappa}$ is ignored,

$$\dot{G}_{\parallel,y}^{(aa,S)} = \pm \tan \theta^{(a)} \dot{I}_{\parallel,[yx]}^{(aa)}, \quad (88)$$

where $\dot{I}_{\parallel,[yx]}^{(aa)}$ is given by Eq. (64); the signs “+” and “−” stand for $a \in i$ and $a \in \alpha$, respectively.

By comparing Eqs. (88) and (81), one can see that $\dot{G}_{\parallel,y}^{(aa,S)}$ is related to IOAM of the a th beam, like $\dot{G}_{\perp,y}^{(aa)}$ is related to the beam’s spin. The scale of both STLMs is Υ .

$\dot{G}_{\parallel,y}^{(aa,B)}(\dot{\mathcal{V}}^{(aa)})$ is calculated in a different way. The integrand in Eq. (85), which is obtained after the replacement $\Omega(\boldsymbol{\kappa}, \tilde{\kappa}) \rightarrow \Omega(\boldsymbol{\kappa}, 0)$, contains the singularity; however, the factor $\Omega(\boldsymbol{\kappa}, 0)$ is independent of the variable $\tilde{\kappa}$. Taking into account this fact, let us first carry out the integration with respect to $\tilde{\kappa}$; this gives the Heaviside step function $\Theta(\pm z^{(a)})$ in the integrand. After that, carrying out the integration with respect to $z^{(a)}$, we get

$$\dot{G}_{\parallel,y}^{(aa,B)}(\dot{\mathcal{V}}^{(aa)}) = \dot{\Gamma}_{\parallel,y}^{(aa)} D_z^{(a)}, \quad (89)$$

where $\dot{\Gamma}_{\parallel,y}^{(aa)}$ and $D_z^{(a)}$ are given by Eqs. (53) and (54) and Eq. (84), respectively.

$\dot{G}_{\parallel,y}^{(aa,B)}(\dot{\mathcal{V}}^{(aa)})$ is proportional to the length of the part of the a th beam confined in the prism $\mathcal{P}^{(aa)}$, so, it represents the bulk TLM. $\Gamma_y^{(ii)} = 0$ [see Eq. (58)]; hence, $G_{\parallel,y}^{(ii,B)}(\mathcal{V}^{(ii)}) = 0$. In the total-reflection regime $G_{\parallel,y}^{(\rho\rho,B)}(\mathcal{V}^{(\rho\rho)}) = 0$ as well. In the partial-reflection regime $\dot{G}_{\parallel,y}^{(\alpha\alpha,B)}(\dot{\mathcal{V}}^{(\alpha\alpha)})$, like $\dot{\Gamma}_{\parallel,y}^{(\alpha\alpha)}$, can have nonzero values. Let us estimate the greatest possible scale of $\dot{G}_{\parallel,y}^{(\alpha\alpha,B)}(\dot{\mathcal{V}}^{(\alpha\alpha)})$ in the latter regime; the estimation can be done on the basis of Eq. (89) and the relation (60). Using these equations and taking into account the expressions for $D_z^{(a)}$ and Υ given by Eqs. (84) and (65), we get that

$$\frac{|\dot{G}_{\parallel,y}^{(\alpha\alpha,B)}| \Lambda}{\Upsilon D_z} = O\left(\frac{\Lambda^2}{b^2}\right). \quad (90)$$

One can see that $|\dot{G}_{\parallel,y}^{(\alpha\alpha,B)}(\dot{\mathcal{V}}^{(\alpha\alpha)})| \ll \Upsilon$ when the condition (74) is fulfilled. So, in the near-field regions of the secondary beams the bulk TLMs can be ignored if TLMs on the order of Υ are under investigation.

Let us now consider TLMs of the second class $G_{\parallel,y}^{(i\rho)}(\mathcal{V}^{(i\rho)})$ and $\ddot{G}_{\parallel,y}^{(\tau\tau)}(\ddot{\mathcal{V}}^{(\tau\tau)})$. When integrating the TLM densities $g_{\parallel,y}^{(i\rho)}(\mathbf{r})$ or $\ddot{g}_{\parallel,y}^{(\tau\tau)}(\mathbf{r})$ over the volume $\mathcal{V}^{(i\rho)}$ or $\ddot{\mathcal{V}}^{(\tau\tau)}$, it is convenient to use the coordinates x , y , and z . In this case, the passage $D_{x,y,z} \rightarrow \infty$ can be made; see the comment [37]. Carrying out after such a passage the integrations first over y and z and then over $\boldsymbol{\kappa}'$ and x , we get that $\dot{G}_{\parallel,y}^{(aa')S}(\dot{\mathcal{V}}^{(aa')S})$, like $\dot{G}_{\parallel,y}^{(aa,S)}(\dot{\mathcal{V}}^{(aa)})$, is

approximately independent of $\dot{\mathcal{V}}^{(aa)}$, and

$$\begin{aligned} \dot{G}_{\parallel,y}^{(aa')} &= \Upsilon \frac{\delta_{a\tau} - 2}{2 \cos \theta^{(i)}} \text{Im} \int \frac{\kappa_y}{\hat{\mathbf{x}} \cdot \mathbf{k}^{(a)}(\boldsymbol{\kappa})} |f(\boldsymbol{\kappa})|^2 \\ &\times q^{(a')}(\boldsymbol{\kappa}) q^{(a)*}(\boldsymbol{\kappa}) [\mathbf{e}^{(a')}(\boldsymbol{\kappa}) \cdot \mathbf{e}^{(a)*}(\boldsymbol{\kappa})] d^2 \boldsymbol{\kappa}. \end{aligned} \quad (91)$$

In the partial-reflection regime the reflection and refraction coefficients as well as $\hat{\mathbf{x}} \cdot \mathbf{k}^{(i)}(\boldsymbol{\kappa})$ are real; therefore $G_{\parallel,y}^{(i\rho)} = 0$ in this regime. In the total-reflection regime $q_x^{(\alpha)}(\boldsymbol{\kappa})$ and $q_y^{(\alpha)}(\boldsymbol{\kappa})$ are complex, while $\hat{\mathbf{x}} \cdot \mathbf{k}^{(\tau)}(\boldsymbol{\kappa})$ is imaginary, so, $\ddot{G}_{\parallel,y}^{(\tau\tau)}$ and $G_{\parallel,y}^{(i\rho)}$ can take nonzero value. Let us estimate their magnitudes. The integral on the right-hand side of Eq. (91) is a dimensionless quantity. Note that the magnitude of the factor $\kappa_y / [\hat{\mathbf{x}} \cdot \mathbf{k}^{(a)}(\boldsymbol{\kappa})]$ is on the order of Λ/b in the actual region of the function $|f(\boldsymbol{\kappa})|^2$. On the basis of this fact, one can conclude that the greatest possible scale of the above integral cannot exceed Λ/b ; as a consequence, the greatest possible scales of every $\dot{G}_{\parallel,y}^{(aa')}$ in the total-reflection regime cannot exceed $\Upsilon \Lambda/b$. But actually the scales of these TLMs are even less than $\Upsilon \Lambda/b$. Indeed, in the zero-order approximation, when the dependence of the quantities $\zeta^{(\tau)}(\boldsymbol{\kappa})$, $q_x^{(a)}(\boldsymbol{\kappa})$, $q_y^{(a)}(\boldsymbol{\kappa})$, and $\hat{\mathbf{x}} \cdot \mathbf{k}^{(a)}(\boldsymbol{\kappa})$ on $\boldsymbol{\kappa}$ is ignored, $\ddot{G}_{\parallel,y}^{(aa')} = 0$; this relation follows from Eq. (59). And meanwhile, the corrections to the aforementioned quantities are small in the actual region of the function $|f(\boldsymbol{\kappa})|^2$; see the relations (30), (31), (33), (34), and (36). Hence, unlike the spin-dependent STLMs, the IOAM-dependent STLMs only of the first class can be on the order of Υ .

STLM in the total space. STLMs in the first and second media will be denoted by $G_{\beta,y}^{(1)}$ and $G_{\beta,y}^{(2)}$, respectively. Bearing in mind the definition (71) and taking into account Eqs. (39) and (40), we get

$$G_{\beta,y}^{(1)} = G_{\beta,y}^{(ii)} + G_{\beta,y}^{(\rho\rho)} + G_{\beta,y}^{(i\rho)} \quad (92)$$

and

$$G_{\beta,y}^{(2)} = G_{\beta,y}^{(\tau\tau)}. \quad (93)$$

Therefore, the spin-dependent or IOAM-dependent STLMs in the second medium are given by Eqs. (78) or (88) for $aa' \in \tau\tau$. These STLMs in the first medium, $G_{\perp,y}^{(1)}$ and $G_{\parallel,y}^{(1)}$, can be calculated by the use of Eqs. (78)–(80) and Eqs. (88), (64)–(67), respectively. Let us also use the relations (17) and (18) and the relations $Q^{(\rho)} + Q^{(\tau)} = 1$ when calculating $G_{\perp,y}^{(1)}$ and $G_{\parallel,y}^{(1)}$, respectively. Then, we get that the spin-dependent or IOAM-dependent STLMs in the first and the second media are related by [38]

$$\epsilon^{(1)} G_{\beta,y}^{(1)} = -\epsilon^{(2)} G_{\beta,y}^{(2)}. \quad (94)$$

The spin-dependent or IOAM-dependent STLM in the total space

$$G_{\beta,y} = G_{\beta,y}^{(1)} + G_{\beta,y}^{(2)}. \quad (95)$$

Substituting $G_{\beta,y}^{(1)}$ obtained by means of Eq. (94) into the right-hand side of Eq. (95) and taking into account Eq. (93), we get

$$G_{\beta,y} = \left(1 - \frac{\epsilon^{(2)}}{\epsilon^{(1)}}\right) G_{\beta,y}^{(\tau\tau)}. \quad (96)$$

The global STLM

$$G_y = G_{\perp,y} + G_{\parallel,y}. \quad (97)$$

VI. THE RELATION BETWEEN STLM AND TShCGs OF THE SECONDARY BEAMS

It is known that there is a relation between the global STLM and TShCGs of the reflected and transmitted light beams. Let us consider this relation.

TShCG of the α th secondary beam, which will be denoted by $h^{(\alpha)}$, is defined as follows:

$$h^{(\alpha)} = Y^{(\alpha)} - Y^{(i)}. \quad (98)$$

Here $Y^{(a)}$ is the y coordinate of the center of gravity of the a th beam of homogeneous plane waves, which is given by

$$Y^{(a)} = \frac{1}{\dot{V}^{(aa)}} \int_{-\infty}^{\infty} dy \int_{\gamma_-^{(a)}}^{\gamma_+^{(a)}} dx^{(a)} y \dot{w}^{(aa)}(\mathbf{r}), \quad (99)$$

where $\dot{w}^{(aa)}(\mathbf{r})$ is the electromagnetic energy density in this beam,

$$\dot{w}^{(aa)}(\mathbf{r}) = \frac{1}{16\pi} [\epsilon^{(a)} |\mathbf{E}^{(a)}(\mathbf{r})|^2 + |\mathbf{H}^{(a)}(\mathbf{r})|^2], \quad (100)$$

and $\dot{V}^{(aa)}$ is the electromagnetic energy *pul* of the beam,

$$\dot{V}^{(aa)} = \int_{-\infty}^{\infty} dy \int_{\gamma_-^{(a)}}^{\gamma_+^{(a)}} dx^{(a)} \dot{w}^{(aa)}(\mathbf{r}). \quad (101)$$

The limits of integration $\gamma_-^{(a)}$ and $\gamma_+^{(a)}$ are given by Eqs. (49) or (50). If the condition (51) is fulfilled, then every finite $\gamma_{\pm}^{(a)}$ can be replaced by $\pm\infty$; in this case $Y^{(a)}$ and $\dot{V}^{(aa)}$, like $\dot{\mathbf{r}}_{\beta}^{(aa)}$ and $\dot{I}^{(aa)}$, are independent of $z^{(a)}$. It is worth noting that $Y^{(a)}$ represents the first normalized moment of the electromagnetic energy distribution in the transverse direction inside the a th beam.

TShCGs of secondary beams as well as STLMs are the dynamical characteristics of the processes of the beam's reflection and transmission. The relation between these quantities can be established, if one mentally selects a rather long sector of the incident beam that is situated far enough from the interface and traces the motion of the packet created in such a way up to the time instant when the secondary packets are far enough from the interface. On the basis of the equation of motion of the center of gravity of the electromagnetic field selected, the following relation can be obtained (see [14,15] and Appendix B):

$$G_y = (Q^{(\rho)} h^{(\rho)} + Q^{(\tau)} h^{(\tau)}) \Gamma_{\parallel,z}^{(ii)}. \quad (102)$$

VII. DISCUSSION OF THE RESULTS AND CONCLUSIONS

General remarks. In this paper the calculations of the surface transverse linear momenta (STLMs) generated during reflection and transmission of a paraxial light beam at a plane interface between two isotropic transparent media have been carried out. Throughout the body of the paper LM was assumed to be the Abraham one.

In order to identify STLMs, TLMs confined in the sufficiently large domains adjacent to the interface have been

calculated. STLMs represent the parts of TLMs that are independent of the domains' dimensions. The following particular TLMs have been investigated: TLMs of the incident, reflected, and transmitted fields as well as the interference TLM in the first medium. They are labeled by the superscripts ii , $\rho\rho$, $\tau\tau$, and $i\rho$, respectively. An arbitrary particular TLM is labeled by the superscript aa' . TLMs in the first and the second medium, which are labeled by the superscripts 1 and 2, as well as TLMs in the total space have also been considered.

Particular TLMs have been classified according two different criteria. First, every particular LM density $\mathbf{g}^{(aa')}(\mathbf{r})$ has been decomposed into two parts [see Eqs. (43)–(47)]; they are labeled by the subscripts \perp and \parallel . TLMs created by the transverse components of these vectors are denoted by $G_{\perp,y}^{(aa')}$ and $G_{\parallel,y}^{(aa')}$, respectively. The former is dependent on the polarization of the incident beam while the surface part of the latter is dependent on the beam's IOAM. In view of that, the respective STLMs are called spin-dependent and IOAM-dependent STLMs.

Second, TLMs have been divided into the following classes: the first class is represented by TLMs in the beams of homogeneous plane waves, and the second class consists of the interference TLM and TLM in inhomogeneous waves that are generated in the second medium at total reflection. Such a division has been made because the features of these TLMs are different. In particular, the scales of effective x dimension of the domains in which STLMs of the first and the second classes exist are different: they are equal to b and $\Lambda = \lambda/(2\pi)$, respectively, where b is the characteristic dimension of the incident beam and λ is the wavelength in the first medium; see Appendix A. TLMs of the first and the second classes are labeled by one dot and two dots over respective letters.

It has been shown that the greatest possible scale of every particular STLM cannot exceed LM confined in the sector of the incident beam of Λ length (the sector is assumed to be situated far from the interface). This quantity was denoted by Υ ; STLMs on such a scale have been investigated in detail. Note that, as the light velocity in vacuum is assumed equal to unity, Υ is equal to Λ times the intensity of the incident beam.

Every particular TLM is equal to zero at normal incidence. Throughout the paper, it is assumed that the angle of incidence $\theta^{(i)} \neq 0$.

The particular IOAM-dependent TLMs. The (aa) th IOAM-dependent STLM of the first class $\dot{G}_{\parallel,y}^{(aa,S)}$ is given by Eq. (88). This equation establishes the relationship between the part of IOAM *pul* of the a th beam and $\dot{G}_{\parallel,y}^{(aa,S)}$; the former is given by Eq. (64). Eventually, $\dot{G}_{\parallel,y}^{(aa,S)}$ is proportional to the factor $L_{[yx]}^{(ii)}$ that is given by Eq. (66); if IOAM of the incident beam is well defined [see Eq. (24)], then $L_{[yx]}^{(ii)} = l/2$, where l is the azimuthal index of the incident beam. The signs of $\dot{G}_{\parallel,y}^{(\rho\rho,S)}$ and $\dot{G}_{\parallel,y}^{(\tau\tau,S)}$ are opposite to the sign of $\dot{G}_{\parallel,y}^{(ii,S)}$.

It is necessary to explain why the value of $\dot{G}_{\parallel,y}^{(aa,S)}$, provided $L_{[yx]}^{(ii)} \neq 0$, is left finite as $b \rightarrow \infty$. Indeed, the greatest possible scale of the density of the IOAM-dependent TLM is Λ/b times the mean value of the density of the axial LM in the incident beam, so, the ratio of these densities as well as the former one tend to zero as $b \rightarrow \infty$. However, the effective x

dimension of the region in which STLM of the first class exists is on the order of b , so, the scale of its volume is b/Λ times the scale of the volume of the sector of the incident beam of Λ length. The combination of the two above ratios enables independence of $\dot{G}_{\parallel,y}^{(aa,S)}$ of b ; see Appendix A.

The greatest possible scale of the density of every particular IOAM-dependent STLM of the second class is the same as this scale of STLM of the first class. However, the scale of the effective x dimension of the region in which the former STLM exists is Λ . As a consequence, the greatest possible scale of $\ddot{G}_{\parallel,y}^{(aa')}$ is $\Upsilon(\Lambda/b)$; see Appendix A. Meanwhile, the quantity $\Upsilon(\Lambda/b)$ is to be considered as the upper estimate of the scale of $\ddot{G}_{\parallel,y}^{(aa')}$. The analysis of the rigorous expression (91) for $\ddot{G}_{\parallel,y}^{(aa')}$ leads to the conclusion that $G_{\parallel,y}^{(i\rho)} = 0$ in the partial-reflection regime, while the scales of $\ddot{G}_{\parallel,y}^{(\tau\tau)}$ and $G_{\parallel,y}^{(i\rho)}$ in the total-reflection regime are much less than $\Upsilon\Lambda/b$.

On the basis of the relationship between $I_{\parallel,[yx]}^{(aa)}$ and $\dot{G}_{\parallel,y}^{(aa)}$, one can come to the conclusion that the appearance of the IOAM-dependent STLM is stipulated by influence of the interface on the rotational energy motion in the a th beam. The detailed analysis of such a mechanism of generation of the particular IOAM-dependent STLM is carried out in Appendix C, where the geometrical interpretation of the IOAM-dependent STLM is presented; the summary is below.

The distribution of 2D planar vector $\dot{\mathbf{g}}_{\parallel,p}^{(aa)}(\mathbf{r})$ [this vector is defined by Eq. (C1)] in every cross section of the a th beam can be represented by the congruence of the curves, the vector $\dot{\mathbf{g}}_{\parallel,p}^{(aa)}(\mathbf{r})$ being the tangent to the respective curve. If the beam's cross section is situated far from the point O, these curves in the actual region of the beam are approximately closed, being circles when IOAM is well defined (O is the point of intersection of the beams axes with the interface; see Fig. 1). In this case, TLM confined in the upper half of the a th beam where $x^{(a)} > 0$ is compensated by TLM confined in its lower half where $x^{(a)} < 0$. Hence, far from the point O, TLM *pul* of the a th beam is approximately equal to zero. On the other hand, if the beam's cross section is near the point O, then a number of $\dot{\mathbf{g}}_{\parallel,p}^{(aa)}$ lines in the actual region of the beam are cut by the interface, see Fig. 4, so, the aforementioned compensation is missing. As a consequence, TLM *pul* of the a th beam is nonzero in the vicinity of the point O; hence, $\dot{G}_{\parallel,y}^{(aa)}$ is nonzero too.

The qualitative geometrical interpretation of the particular IOAM-dependent STLMs that was discussed above can be applied to the real beams. The respective quantitative analysis of these STLMs has been carried out using the model of the incident beam that has been represented by a square cylinder whose axis coincides with the $z^{(i)}$ axis. It was assumed that the electromagnetic field and, as a consequence, $\mathbf{g}_{\parallel,p}^{(ii)}(\mathbf{r})$ are localized on the cylinder's surface. By the use of this model of the incident beam, it can be clearly explained why $\dot{G}_{\parallel,y}^{(aa)}$ is proportional to $I_{\parallel,[yx]}^{(aa)}$. What is surprising is that the expressions for STLMs of the incident and secondary beams derived by the use of such a crude model turned out to be quite similar to ones derived rigorously.

In the partial-reflection regime, TLMs of secondary beams, which are created by the LM densities $g_{\parallel,y}^{(\rho\rho)}(\mathbf{r})$ and $\dot{g}_{\parallel,y}^{(\tau\tau)}(\mathbf{r})$, can also have bulk parts. These are proportional to the lengths

of the selected sectors of secondary beams; see Eq. (89). Note that among all particular TLMs considered only $G_{\parallel,y}^{(\rho\rho)}$ and $\dot{G}_{\parallel,y}^{(\tau\tau)}$ can have the bulk parts; they are connected with the angular transverse shifts of the centers of gravity (TShCGs) of secondary beams [23,25,31,33–36]. In the near-field regions of these beams, which are adjacent to the interface, the bulk TLMs can be ignored, as their scales are much less than Υ ; see Eq. (90). On the other hand, the bulk TLMs can be on the order of Υ or even significantly exceed it in the far-field regions.

The particular spin-dependent STLMs. Every particular TLM created by the TLM density $g_{\perp,y}^{(aa')}(\mathbf{r})$ has no bulk part, while its surface part is given by Eq. (78) and Eq. (79) or (80). $G_{\perp,y}^{(aa')}$ can have nonzero value if $\text{Im}(m^*\Psi^{(aa')}) \neq 0$. The factors m and $\Psi^{(aa')}$ are as follows: m , which is given by Eq. (19), describes the polarization of the incident beam, $\Psi^{(ii)} = 1$, while every other factor $\Psi^{(aa')}$ is the product or the sum of the Fresnel reflection or transmission coefficients. If the incident beam is elliptically polarized, i.e., if the parameter m is complex, then $\text{Im}(m^*\Psi^{(aa')}) \neq 0$ for every combination of the superscripts a and a' ; in this case every $G_{\perp,y}^{(aa')} \neq 0$ in the total-reflection as well as in the partial-reflection regimes. If the incident beam is linearly polarized and the polarization vector is inclined to the plane of incidence, then all $G_{\perp,y}^{(aa')}$, except $G_{\perp,y}^{(ii)}$, are nonzero in the total-reflection regime, while every $G_{\perp,y}^{(aa')} = 0$ in the partial-reflection regime. If the incident beam is $\hat{\mathbf{x}}^{(i)}$ or $\hat{\mathbf{y}}$ polarized, then every $G_{\perp,y}^{(aa')} = 0$ in the both regimes.

Unlike IOAM-dependent STLMs, the particular spin-dependent STLMs of both classes can be on the scale of Υ ; this fact is explained in Appendix A. The particular spin-dependent STLMs of the first class can be on this scale for the same reason as the IOAM-dependent STLMs. Note that $G_{\perp,y}^{(aa)}$ is related to the spin of the a th beam in the same way as $\dot{G}_{\parallel,y}^{(aa,S)}$ is related to the beam's IOAM; compare Eqs. (81) and (88). In view of that, the geometrical interpretation of the IOAM-dependent STLMs presented in Appendix C and summarized above can also be applied to the spin-dependent STLMs of the first class.

The particular spin-dependent STLMs of the second class $\dot{G}_{\perp,y}^{(aa')}$ can be on the scale of Υ for another reason. The scale of the effective x dimension of the regions in which the particular spin-dependent and IOAM-dependent STLMs of the second class exist is the same. However, the greatest possible scale of $\ddot{g}_{\perp,y}^{(aa')}$ is of the order of the mean LM density in the incident beam. So, it is b/Λ times the greatest possible scale of $\ddot{g}_{\parallel,y}^{(aa')}$ as well as of $\dot{g}_{\parallel,y}^{(aa)}$ and $\dot{g}_{\perp,y}^{(aa)}$.

Another distinction between the particular spin-dependent and IOAM-dependent STLMs is that the former, unlike the latter, are independent of the space structure of the incident beam. This distinction is connected with the distinction between the natures of the spin AM and IOAM; see, e.g., [10,12,13]. In view of that, the relation (78) can be applied, in a proper way, to the process of reflection and transmission of a plane wave. In the plane-wave limit, this relationship between LMs can be converted into the relationship

between the respective power flows; see Eq. (82). Comparing Eqs. (78) and (82), one can see that all conclusions made about the particular spin-dependent STLMS can also be applied to the respective spin-dependent transverse power flows (TPFs).

Note that a plane-wave approach has been used in many of previous investigations of the spin-dependent TPFs. In such an approach, $\dot{P}_{\perp,y}^{(\tau\tau)}$ and $P_{\perp,y}^{(i\rho)}$ have been calculated in [2–7,9] and [9], respectively. The results of these calculations coincide with $\dot{P}_{\perp,y}^{(\tau\tau)}$ and $P_{\perp,y}^{(i\rho)}$ given by Eq. (82). On the contrary, the particular spin-dependent TPFs of the first class $\dot{P}_{\perp,y}^{(aa)}$ cannot directly be obtained in the plane-wave approach.

STLM in the total space. Both IOAM-dependent and spin-dependent STLMS in the second medium, $G_{\parallel,y}^{(2)}$ and $G_{\perp,y}^{(2)}$, are STLMS of the transmitted field, $G_{\perp,y}^{(\tau\tau)}$ and $G_{\parallel,y}^{(\tau\tau)}$, while every STLM in the first medium, $G_{\beta,y}^{(1)}$, is the sum of STLMS of the incident and reflected beams as well as the interference STLM. Every $G_{\beta,y}^{(1)}$ is related to $G_{\beta,y}^{(2)}$ by Eq. (94).

The IOAM-dependent or spin-dependent STLM in the total space $G_{\beta,y}$ is related to $G_{\beta,y}^{(\tau\tau)}$ by Eq. (96). It follows from this relationship that the signs of $G_{\beta,y}$ and $G_{\beta,y}^{(\tau\tau)}$ are the same if $\epsilon^{(2)} < \epsilon^{(1)}$, and they are opposite if $\epsilon^{(2)} > \epsilon^{(1)}$. Otherwise, the features of $G_{\beta,y}$ are similar to the features of $G_{\beta,y}^{(\tau\tau)}$ that have been analyzed above. In particular, it follows from this analysis that $G_{\perp,y}$ can be on the scale of Υ in both partial-reflection and total-reflection regimes, while $G_{\parallel,y}$ can be on such a scale only in the partial-reflection regime.

Let us discuss the features of $G_{\parallel,y}$ in more detail and begin with the case of total reflection. In this case $G_{\parallel,y}$, like $\dot{G}_{\parallel,y}^{(\tau\tau)}$, is approximately equal to zero; nevertheless, both STLMS in the first medium are nonzero if $L_{[yx]}^{(ii)} \neq 0$. $G_{\parallel,y} = 0$ in the total-reflection regime because $G_{\parallel,y}^{(ii)}$ is compensated by $G_{\parallel,y}^{(\rho\rho)}$. In the partial-reflection regime there is no such compensation, and the IOAM-dependent STLM in the first medium, which is approximately equal to $G_{\parallel,y}^{(ii)} + G_{\parallel,y}^{(\rho\rho)}$, is nonzero if $L_{[yx]}^{(ii)} \neq 0$. Nevertheless, it can be affirmed that even in this regime only the process of the beam's transmission but not of the beam's reflection is related to the appearance of $G_{\parallel,y}$. Indeed, the intensity of the incident beam can be divided into the part that is to be reflected and the part that is to be transmitted; they are proportional to $Q^{(\rho)}$ and $Q^{(\tau)}$, respectively. It is easy to see that the IOAM-dependent STLM related to the former part, i.e., $Q^{(\rho)}G_{\parallel,y}^{(ii)}$, is compensated by $G_{\parallel,y}^{(\rho\rho)}$.

The relationship between STLM in the total space and TShCGs of secondary beams. Let us now turn to the problem of experimental investigation of STLM. In view of this problem, the relation (102) between the global STLM and the linear combination of TShCGs of the reflected and transmitted light beams is of significant interest, as indirect investigation of STLM is possible on the basis of this relationship. Let us discuss its features. First of all, it should be mentioned that Eq. (102) establishes the relationship between the global STLM and the global TShCGs of secondary beams, the latter being the sum of the spin-dependent and IOAM-dependent TShCGs. However, the spin-dependent and IOAM-dependent effects can easily be divided. For instance, only the former or only the latter effect occurs when the incident beam is the

elliptically polarized Gaussian beam or the $\hat{x}^{(i)}$ - or $\hat{y}^{(i)}$ -polarized Laguerre-Gaussian beam, respectively.

When one secondary beam is generated, i.e., in the case of total reflection or total transmission, then there is an unambiguous connection between $G_{\beta,y}$ and TShCG of the secondary beam. TShCG of this beam is exclusively caused by the electromagnetic energy motion in the transverse direction. Hence, the detection of TShCG of a solitary beam means also the detection of STLM in the total space and, according to the relation (96), the detection of STLM in the second medium. In view of that, it should be mentioned that experimental investigations of the spin-dependent TShCG in the total-reflection regime have been made in a number of works; see, e.g., [6,39] and the references in [16]. On the contrary, the IOAM-dependent TShCG of the totally transmitted light beam has yet not been detected.

In the partial-reflection regime there is no one-to-one correspondence between STLM and TShCG of every secondary beam. In this case there are two mechanisms of generation of TShCGs; these mechanisms for the IOAM-dependent TShCGs have been considered in [40]. So, the global STLM in the partial-reflection regime can be detected if TShCGs of both secondary beams are measured. Note that when STLMS are under investigation in the partial-reflection regime, then the possible appearance of the bulk TLMs should be taken into account; see the discussion of the IOAM-dependent STLMS.

The detailed analysis of TShCGs of secondary beams is not the aim of the present paper. However, in view of their relation to STLMS, the following fact is to be mentioned. It has been concluded that the dependence of $m(\kappa)$, $q_x^{(\alpha)}(\kappa)$, and $q_y^{(\alpha)}(\kappa)$ on κ can be ignored, when STLMS on the scale of Υ are under consideration. However, ignoring such a dependence is impossible when calculating TShCGs of the partially reflected and transmitted beams in the general case. In particular, the spin-dependent TShCG of every secondary beam is the sum of two terms; see Eq. (15) in [24]. The second term in this equation is dependent on the quantity η_y given by Eq. (35). Bearing in mind this fact, it is interesting to discuss the results of investigations of the spin-dependent TShCGs carried out in [41] and [25] from the point of view of the STLM phenomenon. In the aforementioned papers different results for TShCGs of the secondary beams have been obtained. The difference is caused by the fact that different models of the incident beam have been used: η_x and η_y were assumed to be equal to zero in [41], while it was assumed in [25] that the polarization vector is constant across the cross section of the incident beam. In the latter case, the values of η_x and η_y can be nonzero. In view of this distinction, it is remarkable that, as all particular spin-dependent STLMS are approximately independent of η_y , see Eqs. (78)–(80), then they are the same for both aforementioned models of the incident beam provided that m is the same.

The IOAM-dependent TShCGs of the partially reflected and transmitted beams have terms that are proportional to the derivatives of the reflectivity or transmissivity with respect to κ_x ; see Eqs. (14)–(17) in [23]. Meanwhile, the former TShCG has only such a term. These parts of the IOAM-dependent TShCGs are not directly connected with the IOAM-dependent STLMS; this statement is in agreement with the aforementioned analysis of the latter.

If the way of the experimental investigation of the IOAM-dependent STLTM is discussed, then, in addition to TShCGs of secondary beams, the transverse shifts of the optical vortexes with respect to the geometrical optic axes of secondary beams should be taken into account as well. Such a shift among the other effects that accompany the reflection of the beam carrying the vortex has been investigated theoretically and experimentally in [42–44]. It is impossible to directly obtain the relationships between STLMTs and the transverse shifts of the optical vortexes similar to the relation (102). In order to do this, the relationship between the latter and the IOAM-dependent TShCGs of the secondary beams should preliminarily be established. Such a program would be of interest because it is more easy to detect the transverse shift of the optical vortex than TShCG of the beam; see, e.g., [42]. Note that as for the partially reflected beam, the transverse shift of the vortex, like the IOAM-dependent TShCG, is stipulated by the derivatives of the reflectivity with respect to κ [42,44], so, it can be said that the former, like the latter, is not connected with generation of STLTM. In view of this, the investigation of the transverse shifts of the optical vortexes in the transmitted field and establishment of the relationship between these shifts and the IOAM-dependent TShCG of the transmitted beam is of particular interest.

The Minkowski STLTM and the Abraham-Minkowski dilemma. So far, the Abraham STLMTs were under consideration. Let us now briefly discuss the features of the Minkowski STLMTs. As is known, the density of the Minkowski LM is $\epsilon(x)\mathbf{g}(\mathbf{r})$, where $\epsilon(x) = \epsilon^{(1)}$ if $x > 0$, and $\epsilon(x) = \epsilon^{(2)}$ if $x < 0$ (see, e.g., [17–20]). So, the particular Minkowski STLTM, which will be denoted by $\mathcal{G}_{\beta,y}^{(aa')}$, is related to the respective particular Abraham STLTM as follows: $\mathcal{G}_{\beta,y}^{(aa')} = \epsilon^{(a)}G_{\beta,y}^{(aa')}$. Hence, although the values of two particular STLMTs, $G_{\beta,y}^{(aa')}$ and $\mathcal{G}_{\beta,y}^{(aa')}$, are different, their scales, provided that the dielectric constants are not too small and not too large, are equal and their features are similar. The same conclusion is valid for STLMTs in the first and the second media. On the contrary, the features of the Abraham and Minkowski STLMTs in the total space are different. The Minkowski STLMTs in the first and the second media, unlike the Abraham ones, compensate each other; that follows from the above relation and Eq. (94). Hence, the Minkowski STLTM in the total space $\mathcal{G}_{\beta,y}$ is equal to zero in any case.

The STLTM phenomenon seems to be interesting in connection with the Abraham-Minkowski dilemma; see, e.g., the review articles [17–20] and the references therein. The contemporary point of view on this dilemma is as follows: the Minkowski and Abraham LMs represent the canonical and kinetic LMs, respectively; see, e.g., [19,20,45]. The results of direct calculations of STLMTs presented here illustrate this point of view. Indeed, the relation $\mathcal{G}_{\beta,y} = 0$ represents, as a matter of fact, the conservation law for the Minkowski TLM, which is stipulated by the translation invariance of the system under consideration in the transverse direction [14]; note that the aforementioned relation controls the angular transverse shifts of the secondary beams [34]. However, despite that the global Minkowski STLTM is zero, TShCG of the global field can take a nonzero value, as it is the global Abraham STLTM that is related to the energy motion in the transverse direction and, as a consequence, to TShCG of the global field. So, the

specific features of both LMs, the Abraham and Minkowski ones, are manifested in the process under consideration.

ACKNOWLEDGMENTS

The research was supported by the Estonian Institutional Research Funding Project No. IUT2-27 of the Estonian Ministry of Education and Research and by the European Union through the European Regional Development Fund (Project No. 3.2.0101.11-0029).

APPENDIX A: THE SPACE STRUCTURES OF THE PARTICULAR STLMTs

Equations (78)–(80) and (88), (64) represent the results of rigorous calculations of the particular spin-dependent and IOAM-dependent STLMTs, respectively. One can see from these equations that the greatest possible scale of all particular STLMTs of the first class as well as of the particular spin-dependent STLMTs of the second class is Υ . On the contrary, the scales of the particular IOAM-dependent STLMTs of the second class are much less than Υ . In order to elucidate the similarities and distinctions between particular STLMTs, the analysis of their space structures is given below.

In the body of the paper we operated with the well-defined quantities. Unlike there, here we will operate with the scales of these quantities, which can be estimated on the basis of the expressions (44)–(47) for the LM densities. In so doing, the following parameters will be used: Λ , b , and the mean value of $g_{\parallel,z}^{(ii)}(\mathbf{r})$, which will be denoted as $\langle g_{\parallel,z}^{(ii)} \rangle$. The greatest possible scale of a quantity will be denoted by the same letter, which denotes the quantity, but with a line above it.

Let us introduce 1D, 2D, and 3D characteristics of the (aa') th STLTM $X_{\beta}^{(aa')}$, ϱ , and $v_{\beta}^{(aa')}$, respectively. They are defined as follows: $X_{\beta}^{(aa')}$ is the effective x dimension of the region in which the (aa') th STLTM exists, ϱ is the mean area of the spot on the interface, which is illuminated by the incident beam, and $v_{\beta}^{(aa')}$ is the effective volume of the (aa') th STLTM. ϱ is approximately the area of every particular STLTM on the interface, while $X_{\beta}^{(aa')}$ and $v_{\beta}^{(aa')}$ of different STLMTs can be different. $\bar{v}_{\beta}^{(aa')}$ is related to $\bar{\varrho}$ and $\bar{X}_{\beta}^{(aa')}$ by $\bar{v}_{\beta}^{(aa')} = \bar{\varrho}\bar{X}_{\beta}^{(aa')}$. As $\bar{\varrho} = b^2$, then

$$\bar{v}_{\beta}^{(aa')} = b^2\bar{X}_{\beta}^{(aa')}. \quad (\text{A1})$$

The expression for the greatest possible scale of the (aa') th STLTM can be written as follows: $\bar{G}_{\beta,y}^{(aa')} = \bar{v}_{\beta}^{(aa')}\bar{g}_{\beta,y}^{(aa')}$. Substituting Eq. (A1) into the right-hand side of the above equation we get

$$\bar{G}_{\beta,y}^{(aa')} = b^2\bar{X}_{\beta}^{(aa')}\bar{g}_{\beta,y}^{(aa')}. \quad (\text{A2})$$

$\bar{G}_{\beta,y}^{(aa')}$ is to be compared with the scale of Υ . Note that the effective area of the cross section of the incident beam, like ϱ , is on the order of b^2 , so, $\bar{\Gamma}_{\parallel,z}^{(ii)} = b^2\langle g_{\parallel,z}^{(ii)} \rangle$. Υ is given by Eq. (65); hence,

$$\bar{\Upsilon} = b^2\Lambda\langle g_{\parallel,z}^{(ii)} \rangle. \quad (\text{A3})$$

Dividing the left-hand and right-hand sides of Eqs. (A2) and (A3), we get the following relation:

$$\frac{\overline{G}_{\beta,y}^{(aa')}}{\overline{\Upsilon}} = \frac{\overline{X}_{\beta}^{(aa')}}{\Lambda} \frac{\overline{g}_{\beta,y}^{(aa')}}{\langle g_{\parallel,z}^{(ii)} \rangle}. \quad (\text{A4})$$

So, the greatest possible scale of $\overline{G}_{\beta,y}^{(aa')}$ is defined by two ratios $\overline{X}_{\beta}^{(aa')}/\Lambda$ and $\overline{g}_{\beta,y}^{(aa')}/\langle g_{\parallel,z}^{(ii)} \rangle$.

Let us begin with the analysis of the former ratio. The value of $\overline{X}_{\beta}^{(aa')}$ is mainly determined by the value of the scalar product $\hat{\mathbf{x}} \cdot \mathbf{K}_{-}^{(aa')}(\boldsymbol{\kappa}, \boldsymbol{\kappa}')$ in the exponent in the right-hand side of Eq. (44). It is the same for $\beta \in \parallel$ and $\beta \in \perp$; in view of that, $\overline{X}_{\parallel}^{(aa')} = \overline{X}_{\perp}^{(aa')}$. On the other hand, $\overline{X}_{\beta}^{(aa')}$ and $\overline{X}_{\beta}^{(aa')}$ are different, because

$$\mathbf{K}_{-}^{(aa')}(\boldsymbol{\kappa}, \boldsymbol{\kappa}') \cong \zeta^{(a)}(\kappa_x - \kappa'_x)\hat{\mathbf{x}}^{(a)} + (\kappa_y - \kappa'_y)\hat{\mathbf{y}}, \quad (\text{A5})$$

while

$$\ddot{\mathbf{K}}_{-}^{(aa')}(\boldsymbol{\kappa}, \boldsymbol{\kappa}') \cong 2\hat{\mathbf{x}}(\hat{\mathbf{x}} \cdot \mathbf{k}^{(a)*}). \quad (\text{A6})$$

Consider first the values of $\overline{X}_{\beta}^{(\tau\tau)}$ and $\overline{X}_{\beta}^{(i\rho)}$. Note that $|\hat{\mathbf{x}} \cdot \ddot{\mathbf{K}}_{-}^{(aa')}(\boldsymbol{\kappa}, \boldsymbol{\kappa}')|$ is on the order of Λ^{-1} for both STLMs of the second class; however, $\hat{\mathbf{x}} \cdot \mathbf{K}_{-}^{(i\rho)}(\boldsymbol{\kappa}, \boldsymbol{\kappa}')$ is the real number, while $\hat{\mathbf{x}} \cdot \ddot{\mathbf{K}}_{-}^{(\tau\tau)}(\boldsymbol{\kappa}, \boldsymbol{\kappa}')$ is the imaginary number. So, $\ddot{g}_{\beta,y}^{(\tau\tau)}(\mathbf{r})$ attenuates in the $-x$ direction, the attenuation rate being on the order of Λ . In view of that, STLM in the second medium at $n^{(1)} > n^{(2)}$ and $\theta^{(i)} > \theta^{(c)}$ exists in the layer of the thickness $\sim \Lambda$ adjacent to the interface, and the x dimension of this layer evidently represents the value of $\overline{X}_{\beta}^{(\tau\tau)}$. So, $\overline{X}_{\beta}^{(\tau\tau)}/\Lambda = 1$.

The value of $\overline{X}_{\beta}^{(i\rho)}$, unlike of $\overline{X}_{\beta}^{(i\rho)}$, is not evident because $g_{\beta,y}^{(i\rho)}(\mathbf{r})$ oscillates in the x direction with the spatial frequency on the order of Λ^{-1} . Note that the interference STLM exists in the space domain in which the incident and reflected fields overlap; the actual x dimension of this domain is on the order of b . However, b cannot be considered as $\overline{X}_{\beta}^{(i\rho)}$, because the number of oscillations of $g_{\beta,y}^{(i\rho)}(\mathbf{r})$ in the aforementioned domain is large, being on the order of b/Λ . Note that $\ddot{X}_{\beta}^{(\tau\tau)}$ can rigorously be defined through the second moment of the $\ddot{g}_{\beta,y}^{(\tau\tau)}(\mathbf{r})$ distribution in the x direction. Let us define $X_{\beta}^{(i\rho)}$ in the same way, namely, as follows: if $G_{\beta,y}^{(i\rho)} \neq 0$, then

$$X_{\beta}^{(i\rho)} = \sqrt{\frac{1}{|G_{\beta,y}^{(i\rho)}|} \left| \int x^2 g_{\beta,y}^{(i\rho)}(\mathbf{r}) d^3\mathbf{r} \right|}. \quad (\text{A7})$$

The integration on the right-hand side of Eq. (A7) is carried out over the volume $\mathcal{V}^{(i\rho)}$. Substituting Eq. (44) into the right-hand side of Eq. (A7) and carrying out the subsequent integrations with respect to \mathbf{r} and $\boldsymbol{\kappa}'$ we get that $\overline{X}_{\beta}^{(i\rho)} = \Lambda$.

Hence, one can conclude that although the dependence of the interference STLM on x differs from that of STLM in the second medium at total reflection, nevertheless,

$$\frac{\overline{X}_{\beta}^{(aa')}}{\Lambda} = 1 \quad (\text{A8})$$

for both STLMs of the second class.

As for the (aa) th STLM of the first class, it occurs in the region in which a part of the a th beam of homogeneous plane waves is cut by the interface. The actual x dimension of this region, like the actual x dimension of the interference domain, is on the order of b . The scalar product $\hat{\mathbf{x}} \cdot \mathbf{K}_{-}^{(aa')}(\boldsymbol{\kappa}, \boldsymbol{\kappa}')$, like $\hat{\mathbf{x}} \cdot \mathbf{K}_{-}^{(i\rho)}(\boldsymbol{\kappa}, \boldsymbol{\kappa}')$, is real; however, as follows from Eq. (A5), the scale of the former, unlike of the latter, is b^{-1} in the actual region of κ_x and κ'_x . Hence, the density of STLM of the first class, unlike the density of the interference STLM, changes smoothly in the x direction, the spatial frequency of a possible oscillation being on the order of b^{-1} . In view of that, the value of $\overline{X}_{\beta}^{(aa')}$ is evidently equal to b , so,

$$\frac{\overline{X}_{\beta}^{(aa')}}{\Lambda} = \frac{b}{\Lambda}. \quad (\text{A9})$$

Consider now the ratio $\overline{g}_{\beta,y}^{(aa')}/\langle g_{\parallel,z}^{(ii)} \rangle$. It can easily be verified that the comparison of $\langle g_{\parallel,z}^{(ii)} \rangle$ and $\overline{g}_{\beta,y}^{(aa')}$ comes down to the comparison of the scales of the respective components of the vectors $\mathbf{K}_{+}^{(aa')}(\boldsymbol{\kappa}, \boldsymbol{\kappa}')$ and $\mathbf{K}_{-}^{(aa')}(\boldsymbol{\kappa}, \boldsymbol{\kappa}')$ on the right-hand sides of Eqs. (45) or (46). The components to be compared are as follows: the $z^{(i)}$ component of the vector $\mathbf{K}_{+}^{(ii)}(\boldsymbol{\kappa}, \boldsymbol{\kappa}')$ for $\langle g_{\parallel,z}^{(ii)} \rangle$, the y component of the vector $\mathbf{K}_{+}^{(aa')}(\boldsymbol{\kappa}, \boldsymbol{\kappa}')$ for $\overline{g}_{\parallel,y}^{(aa')}$, and $2D$ vector $\hat{\mathbf{y}} \times \mathbf{K}_{-}^{(aa')}(\boldsymbol{\kappa}, \boldsymbol{\kappa}')$ for $\overline{g}_{\beta,y}^{(aa')}$. Let us determine every ratio $\overline{g}_{\beta,y}^{(aa')}/\langle g_{\parallel,z}^{(ii)} \rangle$ in such a way.

In the zero-order approximation with respect to Λ/b ,

$$\hat{\mathbf{z}}^{(i)} \cdot \mathbf{K}_{+}^{(ii)}(\boldsymbol{\kappa}, \boldsymbol{\kappa}') = 2k_z^{(i)} = 2/\Lambda. \quad (\text{A10})$$

$\hat{\mathbf{y}} \cdot \mathbf{K}_{+}^{(aa')}(\boldsymbol{\kappa}, \boldsymbol{\kappa}') = \kappa_y + \kappa'_y$ in any regime, the partial-reflection and total-reflection ones, and for any a and a' . Then, taking into account the relations (A10) and (30), one can conclude that

$$\frac{\overline{g}_{\parallel,y}^{(aa')}}{\langle g_{\parallel,z}^{(ii)} \rangle} = \frac{\Lambda}{b}. \quad (\text{A11})$$

This relation is valid for the IOAM-dependent STLMs of both classes.

The scale of $\hat{\mathbf{y}} \times \mathbf{K}_{-}^{(aa')}(\boldsymbol{\kappa}, \boldsymbol{\kappa}')$, unlike that of $\hat{\mathbf{y}} \cdot \mathbf{K}_{+}^{(aa')}(\boldsymbol{\kappa}, \boldsymbol{\kappa}')$, is different for STLMs of the first and second classes; as a consequence, the ratios $\overline{g}_{\perp,y}^{(aa')}/\langle g_{\parallel,z}^{(ii)} \rangle$ and $\overline{g}_{\perp,y}^{(aa')}/\langle g_{\parallel,z}^{(ii)} \rangle$ are different too. Taking into account the aforementioned reasonings as well as Eqs. (A5), (A10), and (30), we get

$$\frac{\overline{g}_{\perp,y}^{(aa')}}{\langle g_{\parallel,z}^{(ii)} \rangle} = \frac{\Lambda}{b}. \quad (\text{A12})$$

On the other hand, it follows from Eqs. (A6) and (A10) that

$$\frac{\overline{g}_{\perp,y}^{(aa')}}{\langle g_{\parallel,z}^{(ii)} \rangle} = 1. \quad (\text{A13})$$

The greatest possible scale of every STLM can be determined if one substitutes the expression for the ratio $\overline{X}_{\beta}^{(aa')}/\Lambda$ given by Eq. (A8) or Eq. (A9) and the expression for the ratio $\overline{g}_{\beta,y}^{(aa')}/\langle g_{\parallel,z}^{(ii)} \rangle$ given by one of the equations (A11)–(A13) into

the right-hand side of Eq. (A4). One can see that the greatest possible scale of the spin-dependent STLMs of both classes is $\bar{\Upsilon}$, while the IOAM-dependent STLMs only of the first class can be on such a scale. The values of these STLMs are left finite as $b \rightarrow \infty$. On the contrary, the greatest possible scale of the IOAM-dependent STLMs of the second class is $(\Lambda/b)\bar{\Upsilon}$, so, the values of these STLMs tend to zero as $b \rightarrow \infty$.

Let us summarize the results of the analysis presented. The aforementioned characteristics of the spin-dependent and IOAM-dependent STLMs of the first class are similar. $\bar{g}_{\beta,y}^{(aa)}/\langle g_{\parallel,z}^{(ii)} \rangle = \Lambda/b$ for every β . Hence, $\bar{g}_{\beta,y}^{(aa)} \rightarrow 0$ as $b \rightarrow \infty$; however, STLMs of the first class are left finite because $\bar{X}_{\beta}^{(aa)} \rightarrow \infty$ as $b \rightarrow \infty$. As for STLMs of the second class, both $\bar{X}_{\perp}^{(aa')}$ and $\bar{X}_{\parallel}^{(aa')}$ are independent of b , being equal to Λ . However, $\bar{g}_{\perp,y}^{(aa')}$ and $\bar{g}_{\parallel,y}^{(aa')}$ are different: the former is equal to $\langle g_{\parallel,z}^{(ii)} \rangle$, while the latter is equal to $\langle g_{\parallel,z}^{(ii)} \rangle \Lambda/b$. Just due to this difference, the greatest possible scales of the spin-dependent and IOAM-dependent STLMs of the second class are different, and the latter can be ignored, when STLMs that are on the scale of $\bar{\Upsilon}$ are under consideration.

APPENDIX B: THE REFLECTION AND TRANSMISSION OF A WAVE PACKET

Let us mentally separate a sector of the incident beam, which is restricted with two cross sections. The sector's length will be denoted by \mathcal{D} , and the axial coordinate of its center by $Z^{(i)}$, $Z^{(i)} < 0$. Let us assume that the values of \mathcal{D} and $Z^{(i)}$ satisfy the following conditions:

$$b^2/\Lambda \gg |Z^{(i)}| \gg \mathcal{D} \gg b. \quad (\text{B1})$$

If these conditions are fulfilled, then the influence of the second medium on the selected sector of the incident beam can be ignored.

Being separated from the beam, the selected sector represents a wave packet. Let us investigate the motion of such a packet during the time interval $t_f - t_0$, where t_0 and t_f are the initial and final instants of time. This process is shown schematically in Fig. 3.

The instant of time t_0 will be set equal to $n^{(1)}Z^{(i)}$. In such a setting, the center of the packet would be at the point O at $t = 0$, if the packet were in the homogeneous medium with the refractive index $n^{(1)}$ (note that $1/n^{(1)}$ is the group velocity in the first medium). As for t_f , this instant of time will be assumed to obey the following constraints:

$$b^2/\Lambda \gg t_f/n^{(1)} \gg \mathcal{D}. \quad (\text{B2})$$

If these conditions, which are similar to the conditions (B1), are fulfilled, then the influence of the second medium on the reflected packet and of the first medium on the transmitted packet can be ignored at $t = t_f$. Again, due to the left relations (B1) and (B2), the secondary packets approximately coincide at this instant of time with the respective sectors of secondary beams.

The packets' characteristics will be denoted by the same letters as the beams' ones; however, these letters will be marked by the tilde and their dependence on t will be pointed out.

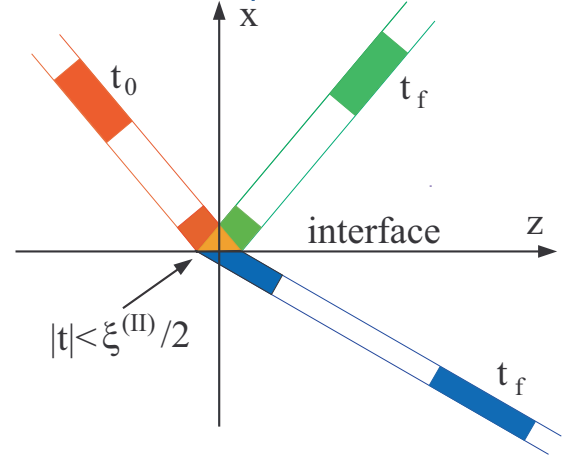


FIG. 3. The scheme of evolution of the selected sector of the incident beam. The red, green, and blue areas depict the sectors of the incident, reflected, and transmitted beams, respectively. The brown area is the interference region. The symbolic borders of the beams are marked by the thin colored lines. $n^{(1)} > n^{(2)}$, $\theta^{(i)} < \theta^{(c)}$.

The relationships between the complex amplitudes of the packets' field vectors $\tilde{\mathbf{E}}^{(a)}(\mathbf{r};t)[\tilde{\mathbf{H}}^{(a)}(\mathbf{r};t)]$, $\tilde{\mathbf{E}}^{(1,2)}(\mathbf{r};t)[\tilde{\mathbf{H}}^{(1,2)}(\mathbf{r};t)]$, and $\tilde{\mathbf{E}}(\mathbf{r};t)[\tilde{\mathbf{H}}(\mathbf{r};t)]$ are the same as the respective relationships between the complex amplitudes of the beams' field vectors $\mathbf{E}^{(a)}(\mathbf{r})[\mathbf{H}^{(a)}(\mathbf{r})]$, $\mathbf{E}^{(1,2)}(\mathbf{r})[\mathbf{H}^{(1,2)}(\mathbf{r})]$, and $\mathbf{E}(\mathbf{r})[\mathbf{H}(\mathbf{r})]$; see Eqs. (26)–(28). The packets' LM densities $\tilde{\mathbf{g}}^{(aa')}(\mathbf{r};t)$, $\tilde{\mathbf{g}}^{(1,2)}(\mathbf{r};t)$, and $\tilde{\mathbf{g}}(\mathbf{r};t)$ are defined by the right-hand sides of Eqs. (38)–(42), if the vectors $\mathbf{E}^{(a)}(\mathbf{r})[\mathbf{H}^{(a)}(\mathbf{r})]$ and $\mathbf{E}^{(1,2)}(\mathbf{r})[\mathbf{H}^{(1,2)}(\mathbf{r})]$ in Eqs. (41) and (42) are replaced by the vectors $\tilde{\mathbf{E}}^{(a)}(\mathbf{r};t)[\tilde{\mathbf{H}}^{(a)}(\mathbf{r};t)]$ and $\tilde{\mathbf{E}}^{(1,2)}(\mathbf{r};t)[\tilde{\mathbf{H}}^{(1,2)}(\mathbf{r};t)]$.

Let us consider the motion of the center of gravity of the electromagnetic field separated as above. Its y component is defined as follows:

$$\tilde{Y}(t) = \frac{1}{\tilde{W}} \int y \tilde{w}(\mathbf{r};t) d^3\mathbf{r}, \quad (\text{B3})$$

where $\tilde{w}(\mathbf{r};t)$ is the electromagnetic energy density given by

$$\tilde{w}(\mathbf{r};t) = \frac{1}{16\pi} [\epsilon(x)|\tilde{\mathbf{E}}(\mathbf{r};t)|^2 + |\tilde{\mathbf{H}}(\mathbf{r};t)|^2] \quad (\text{B4})$$

and

$$\tilde{W} = \int \tilde{w}(\mathbf{r};t) d^3\mathbf{r}; \quad (\text{B5})$$

$\epsilon(x) = \epsilon^{(1)}$ if $x > 0$, and $\epsilon(x) = \epsilon^{(2)}$ if $x < 0$. The integration on the right-hand sides of Eqs. (B3) and (B5) is carried out over the whole space.

$\tilde{w}(\mathbf{r};t)$ obeys a continuity equation

$$\frac{\partial \tilde{w}(\mathbf{r};t)}{\partial t} = -\nabla \cdot \tilde{\mathbf{p}}(\mathbf{r};t), \quad (\text{B6})$$

where ∇ is the gradient operator and $\tilde{\mathbf{p}}(\mathbf{r};t)$ is the Poynting vector. Carrying out the integration of the left-hand and right-hand sides of Eq. (B6) over the whole space, one can verify that the global electromagnetic energy \tilde{W} is the invariant of the motion.

Let us denote by $\tilde{Y}^{(i)}(t_0)$ and $\tilde{Y}^{(\alpha)}(t_f)$ the transverse components of the centers of gravity of the incident packet and of the α th secondary packet at the initial and final time instants, respectively. In what follows, the common denotation t_a for t_0 and t_f will be used: $a \in \{i, \rho, \tau\}$ and $t_i = t_0$, $t_\alpha = t_f$. Then every $\tilde{Y}^{(a)}(t_a)$ reads

$$\tilde{Y}^{(a)}(t_a) = \frac{1}{\tilde{W}^{(aa)}(t_a)} \int y \tilde{w}^{(aa)}(\mathbf{r}; t_a) d^3 \mathbf{r}, \quad (\text{B7})$$

where $\tilde{w}^{(aa)}(\mathbf{r}; t_a)$ is the electromagnetic energy density in the a th packet of the homogeneous plane waves,

$$\tilde{w}^{(aa)}(\mathbf{r}; t_a) = \frac{1}{16\pi} (\epsilon^{(a)} |\tilde{\mathbf{E}}^{(a)}(\mathbf{r}; t_a)|^2 + |\tilde{\mathbf{H}}^{(a)}(\mathbf{r}; t_a)|^2), \quad (\text{B8})$$

and $\tilde{W}^{(aa)}(t_a)$ is the packet's energy at $t = t_a$,

$$\tilde{W}^{(aa)}(t_a) = \int \tilde{w}^{(aa)}(\mathbf{r}; t_a) d^3 \mathbf{r}. \quad (\text{B9})$$

The integration on the right-hand sides of Eqs. (B7) and (B9) is carried out over the upper half space if $a \in \{i, \rho\}$, or over the lower half space if $a \in \tau$.

At $t = t_0$ only the incident packet exists; hence,

$$\tilde{Y}(t_0) = \tilde{Y}^{(i)}(t_0). \quad (\text{B10})$$

At $t = t_f$ only secondary packets exist. At this instant of time $\tilde{W}^{(\rho\rho)}(t_f) + \tilde{W}^{(\tau\tau)}(t_f) = \tilde{W}$, and $\tilde{Y}(t_f)$ can be expressed through $\tilde{Y}^{(\rho)}(t_f)$ and $\tilde{Y}^{(\tau)}(t_f)$ as follows:

$$\tilde{Y}(t_f) = \tilde{Q}^{(\rho)} \tilde{Y}^{(\rho)}(t_f) + \tilde{Q}^{(\tau)} \tilde{Y}^{(\tau)}(t_f), \quad (\text{B11})$$

where $\tilde{Q}^{(\alpha)} = \tilde{W}^{(\alpha\alpha)}(t_f)/\tilde{W}$.

The motion of the center of gravity of the global electromagnetic field in the transverse direction is described by the transverse component of the packet's velocity, which is $d\tilde{Y}(t)/dt$. Let us substitute Eq. (B3) into this expression and use Eq. (B6) as well as the relation $\tilde{\mathbf{p}}(\mathbf{r}; t) = \tilde{\mathbf{g}}(\mathbf{r}; t)$. Then carrying out the integration over y by parts and taking into account the continuity of the component $\hat{\mathbf{x}} \cdot \tilde{\mathbf{g}}(\mathbf{r}; t)$ at the interface, we get

$$\frac{d\tilde{Y}(t)}{dt} = \frac{\tilde{G}_y(t)}{\tilde{W}}, \quad (\text{B12})$$

where

$$\tilde{G}_y(t) = \int \tilde{g}_y(\mathbf{r}; t) d^3 \mathbf{r}. \quad (\text{B13})$$

The integration in Eq. (B13), like in Eqs. (B3) and (B5), is carried out over the whole space, so, $\tilde{G}_y(t)$ is TLM of the global electromagnetic field at the time instant t .

Let us carry out the integration of both parts of Eq. (B12) over the time interval $t_f - t_0$ and take into account Eqs. (B10) and (B11). Then we get the following relation:

$$\tilde{Q}^{(\rho)} \tilde{h}^{(\rho)} + \tilde{Q}^{(\tau)} \tilde{h}^{(\tau)} = \frac{\tilde{\Xi}_y}{\tilde{W}}, \quad (\text{B14})$$

where

$$\tilde{h}^{(\alpha)} = \tilde{Y}^{(\alpha)}(t_f) - \tilde{Y}^{(i)}(t_0) \quad (\text{B15})$$

and

$$\tilde{\Xi}_y = \int_{t_0}^{t_f} \tilde{G}_y(t) dt. \quad (\text{B16})$$

$\tilde{h}^{(\alpha)}$ is TShCG of the respective secondary packet, which the packet has got by the time t_f , and $\tilde{\Xi}_y$ is the action of the global TLM during the time interval $(t_f - t_0)$.

Equation (B14) establishes the relation between the characteristics of the dynamical field; however, it can be converted into the relation (102) between the characteristics of the static field. In order to do this, let us consider three time intervals: the interval I when the incident beam moves in the first medium without contact with the interface, the interval II when the electromagnetic field is in contact with the interface, and the interval III when the secondary beams move in the respective media without contact with the interface. The durations of these intervals and the actions of $\tilde{G}_y(t)$ during them will be denoted by $\xi^{(I)}$, $\xi^{(II)}$, $\xi^{(III)}$ and $\tilde{\Xi}_y^{(I)}$, $\tilde{\Xi}_y^{(II)}$, $\tilde{\Xi}_y^{(III)}$, respectively.

During the time intervals $\xi^{(I)}$ and $\xi^{(III)}$ the incident or secondary packets move as if in the homogeneous media with the refractive indices $n^{(1)}$ or $n^{(2)}$. $\tilde{G}_y(t)$ in these intervals is approximately constant. Namely, $\tilde{G}_y(t) \cong \tilde{G}_y^{(ii)}(t_0)$ during the time interval $\xi^{(I)}$, and $\tilde{G}_y(t) \cong \tilde{G}_y^{(\rho\rho)}(t_f) + \tilde{G}_y^{(\tau\tau)}(t_f)$ during the time interval $\xi^{(III)}$. Here $\tilde{G}_y^{(aa)}(t_a)$ is TLM of the a th packet at the time instant t_a ; this quantity is defined by the right-hand side of Eq. (B13) if the integrand $\tilde{g}_y(\mathbf{r}; t)$ there is replaced by $\tilde{g}_y^{(aa)}(\mathbf{r}; t_a)$ and the integration is carried out over the respective half space. Next, as $|t_a| \gg \mathcal{D}$, then $\xi^{(I)} \cong |t_0|$ and $\xi^{(III)} \cong t_f$. So, $\tilde{\Xi}_y^{(I)} \cong \tilde{G}_y^{(ii)}(t_0)|t_0|$ and $\tilde{\Xi}_y^{(III)} \cong [\tilde{G}_y^{(\rho\rho)}(t_f) + \tilde{G}_y^{(\tau\tau)}(t_f)]t_f$. The packets' characteristics $\tilde{\Xi}_y^{(I)}$ and $\tilde{\Xi}_y^{(III)}$ can be expressed through the beams' characteristics. At $t = t_0$ the incident packet is the sector of the incident beam; hence, $\tilde{G}_y^{(ii)}(t_0) \cong \Gamma_{\parallel, y}^{(ii)} \mathcal{D}$. As $\Gamma_{\parallel, y}^{(ii)} = 0$, see Eq. (58), then $\tilde{\Xi}_y^{(I)} = 0$ as well. $\tilde{\Xi}_y^{(III)}$ describes the action of the global bulk TLM during the time interval $\xi^{(III)}$. In order to estimate its value, let us take into account that the α th secondary packet approximately coincides during the time interval $\xi^{(III)}$ with the sector of the α th beam of $(n^{(1)}/n^{(\alpha)})\mathcal{D}$ length. In view of that, $\tilde{G}_y^{(\alpha\alpha)}(t_f) \cong (n^{(1)}/n^{(\alpha)})\Gamma_y^{(\alpha\alpha)}\mathcal{D}$ and, as a consequence,

$$\tilde{\Xi}_y^{(III)} \cong \left(\Gamma_y^{(\rho\rho)} + \frac{n^{(1)}}{n^{(2)}} \Gamma_y^{(\tau\tau)} \right) \mathcal{D} t_f. \quad (\text{B17})$$

Let us now turn to the time interval $\xi^{(II)}$. As $\mathcal{D} \gg b$, then $\xi^{(II)} \cong n^{(1)}\mathcal{D}$. Next, due to the above condition, the leading and trailing edges of the incident and secondary packets do not contact the interface during the main part of $\xi^{(II)}$. As a consequence, $\tilde{G}_y(t)$ is approximately constant during the time interval $\xi^{(II)}$ and it approximately coincides with the global static STLM. So, the action of the global STLM during this interval

$$\tilde{\Xi}_y^{(II)} \cong n^{(1)} G_y \mathcal{D}. \quad (\text{B18})$$

Let us compare the magnitudes of the actions $\tilde{\Xi}_y^{(II)}$ and $\tilde{\Xi}_y^{(III)}$. G_y is given by Eq. (97). Taking into account this equation as well as Eqs. (64), (78), (88), and (95), we can see that the scale of $\tilde{\Xi}_y^{(II)}$ is $\Upsilon \mathcal{D}$. In the total-reflection regime

$\tilde{\Xi}_y^{(III)} = 0$ because $\Gamma_y^{(\rho\rho)} = 0$, while the scale of $\tilde{\Xi}_y^{(III)}$ in the partial-reflection regime can be estimated on the basis of Eq. (B17). Taking into account this equation as well as the relation (60) and the left relation (B2), we can conclude that the scale of $\tilde{\Xi}_y^{(III)}$ is much less than $\Upsilon\mathcal{D}$; this conclusion is similar to the conclusion made in the passage that follows Eq. (89).

So, the numerator $\tilde{\Xi}_y$ on the right-hand side of Eq. (B14) can be replaced by $\tilde{\Xi}_y^{(II)}$ given by Eq. (B18). In order to calculate the denominator in this expression, let us take into account that $\tilde{W} = \tilde{W}^{(ii)}(t_0)$. As the incident packet represents a section of the incident beam, then $\tilde{W}^{(ii)}(t_0) \cong V^{(ii)}\mathcal{D}$, where $V^{(ii)}$ is given by Eq. (101). Next, $V^{(ii)} = n^{(1)}\Gamma_{\parallel,z}^{(ii)}$, so, $\tilde{W} \cong n^{(1)}\Gamma_{\parallel,z}^{(ii)}\mathcal{D}$. Furthermore, if the packets are approximately the sections of the respective beams at $t = t_a$, then the packets' characteristics $\tilde{Y}^{(a)}(t_a)$ and $\tilde{Q}^{(a)}$ on the left-hand side of Eq. (B14) can be replaced by the respective beams' characteristics $Y^{(a)}$ and $Q^{(a)}$. Once the aforementioned replacements in Eq. (B14) are made, this relation transforms into the relation (102).

APPENDIX C: THE GEOMETRICAL INTERPRETATION OF THE PARTICULAR IOAM-DEPENDENT STLMs

The relation (88) admits a simple geometrical interpretation of the particular IOAM-dependent STLM. It is based on the analysis of the IOAM-dependent rotational energy motion in the beam of the homogenous plane waves, which occurs in a restricted medium. Such a motion within the a th beam can be described by the 2D vector perpendicular to the beam's axis,

$$\dot{\mathbf{g}}_{\parallel,p}^{(aa)}(\mathbf{r}) = \dot{\mathbf{g}}_{\parallel}^{(aa)}(\mathbf{r}) - [\hat{\mathbf{z}}^{(a)} \cdot \dot{\mathbf{g}}_{\parallel}^{(aa)}(\mathbf{r})]\hat{\mathbf{z}}^{(a)}. \quad (\text{C1})$$

Let us first investigate this motion within the incident beam assuming for the sake of simplicity that the beam's IOAM is well defined, i.e., that the beam is characterized by the azimuthal index l ; see Eq. (24). In order to exclude the spin-dependent effects from consideration, it will also be assumed in this Appendix that $\hat{\mathbf{e}}^{(i)} = \hat{\mathbf{x}}^{(i)}$ or $\hat{\mathbf{e}}^{(i)} = \hat{\mathbf{y}}^{(i)}$; in this case $\mathbf{g}_{\perp}^{(ii)}(\mathbf{r}) \cong 0$.

Let us denote by $\Pi(z^{(i)})$ the $(x^{(i)}y)$ plane whose axial coordinate is $z^{(i)}$. The distribution of the planar vector $\mathbf{g}_{\parallel,p}^{(ii)}(\mathbf{r})$ in every plane $\Pi(z^{(i)})$ can be represented by the family of curves, the vector $\mathbf{g}_{\parallel,p}^{(ii)}(\mathbf{r})$ being the tangent to the respective curve; such curves will be called the $\mathbf{g}_{\parallel,p}^{(ii)}$ lines. Further on, the actual region of the beam, where $|\mathbf{r}_p^{(i)}| \sim b$, will be under consideration; the radial component of the vector $\mathbf{g}_{\parallel,p}^{(ii)}(\mathbf{r})$ can be ignored in this region.

Let us introduce a beam whose field vectors are given by Eqs. (3) and (4) for $a \in i$, but which propagates in the homogeneous medium with the dielectric constant $\epsilon^{(1)}$; it will be called a virtual incident beam. The LM density in the virtual beam will be denoted by $\mathbf{g}_{\parallel,p}^{(ii,\circ)}(\mathbf{r}_p^{(i)})$; this vector is approximately independent of $z^{(i)}$ in the near-field region defined by Eq. (73).

The $\mathbf{g}_{\parallel,p}^{(ii,\circ)}$ lines, which depict the distribution of the vector $\mathbf{g}_{\parallel,p}^{(ii,\circ)}(\mathbf{r}_p^{(i)})$ on $\Pi(z^{(i)})$, are approximately closed in the actual region, being the circles if IOAM of the beam is assumed to be well defined. In Fig. 4, these curves are represented by red dashed circles; the arrowed red lines show the directions of the vector $\mathbf{g}_{\parallel,p}^{(ii,\circ)}(\mathbf{r}_p^{(i)})$ in the respective points on $\Pi(z^{(i)})$.

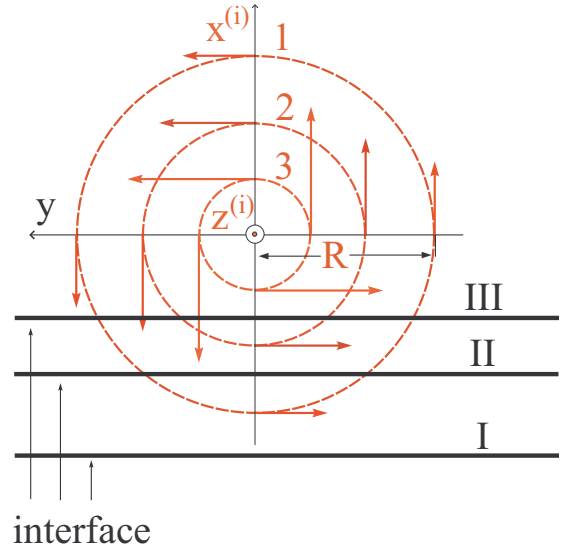


FIG. 4. The $\mathbf{g}_{\parallel,p}^{(ii,\circ)}$ lines in a cross section of the incident beam and possible positions of the interface relative to these lines. $l > 0$.

The relation between the vectors $\mathbf{g}_{\parallel,p}^{(ii,\circ)}(\mathbf{r}_p^{(i)})$ and $\mathbf{g}_{\parallel,p}^{(ii)}(\mathbf{r})$ is as follows:

$$\mathbf{g}_{\parallel,p}^{(ii)}(\mathbf{r}) = \mathbf{g}_{\parallel,p}^{(ii,\circ)}(\mathbf{r}_p^{(i)})\Theta(x^{(i)} - \mathcal{X}^{(i)}(z^{(i)})), \quad (\text{C2})$$

where $\mathcal{X}^{(i)}(z^{(i)})$ is the $x^{(i)}$ coordinate of the interface in the plane $\Pi(z^{(i)})$, which is given by $\mathcal{X}^{(i)}(z^{(i)}) = z^{(i)} \cot \theta^{(i)}$. The property of the vector $\mathbf{g}_{\parallel,p}^{(ii)}(\mathbf{r})$ defined by Eq. (C2) is illustrated in Fig. 4: some $\mathbf{g}_{\parallel,p}^{(ii)}$ lines, like the $\mathbf{g}_{\parallel,p}^{(ii,\circ)}$ lines, are the circles, while the other ones are the upper segments of the circles.

Let us mentally select a part of the virtual incident beam whose shape is the pipe of the diameter $2R$ and assume that the thickness of the pipe's side is small in comparison with R . Like the $\mathbf{g}_{\parallel,p}^{(ii,\circ)}$ line, the projection of the pipe on $\Pi(z^{(i)})$ is represented by the circle; let it be the red dotted circle 1 in Fig. 4.

TLMs *pul* of the real and virtual incident beams, which are confined in the pipe selected, will be denoted by $\sigma_{\parallel,R}^{(ii)}(z^{(i)})$ and $\sigma_{\parallel,R}^{(ii,\circ)}$, respectively. The latter is approximately independent of $z^{(i)}$, and it is evident that $\sigma_{\parallel,R}^{(ii,\circ)} = 0$. It can be said that this relation takes place because TLM confined in the upper half of the pipe selected is compensated by TLM confined in its lower half.

If

$$-z^{(i)} > R \tan \theta^{(i)}, \quad (\text{C3})$$

i.e., if $-\mathcal{X}^{(i)}(z^{(i)}) > R$, then the interface's projection on $\Pi(z^{(i)})$ does not touch the cross section of the pipe with the diameter $2R$. In Fig. 4, such a situation is illustrated by the position of the thick black line I relative to the circle 1: the former does not intersect the latter. So, $\sigma_{\parallel,R}^{(ii)}(z^{(i)}) = \sigma_{\parallel,R}^{(ii,\circ)} = 0$ in the above region of $z^{(i)}$. On the contrary, if

$$|z^{(i)}| < R \tan \theta^{(i)}, \quad (\text{C4})$$

i.e., if $|\mathcal{X}^{(i)}(z^{(i)})| < R$, then the lower segment of the circle 1 is cut by the thick black line; in Fig. 4, this situation is illustrated by the positions of the thick black lines II and III relative

the circle 1. This means that in the region of $z^{(i)}$ defined by Eq. (C4) the interface cuts a lower part of the pipe considered. So, TLM *pul* of the pipe, which is located in the upper pipe's half, is not compensated by that located in the lower half, and, as a consequence, $\sigma_{\parallel,R}^{(ii)}(z^{(i)}) \neq 0$ in this region. The incident beam can be represented as the sum of the pipes of different radii. Applying the above arguments to every pipe one can conclude that TLM *pul* of the incident beam is essentially nonzero in the region in which $|z^{(i)}| \sim b \tan \theta^{(i)}$, and, for this reason, $G_{\parallel,y}^{(ii)} \neq 0$ as well.

The analysis of TLMs of the secondary beams can be carried out in a similar way. So, it can be said that the IOAM-dependent STLM of an arbitrary beam $\hat{G}_{\parallel,y}^{(aa)}$ occurs because the part of this beam adjacent to the interface is cut by the latter.

In the previous part of this Appendix the qualitative explanation of the mechanism of generation of the IOAM-dependent STLM of the a th beam has been given. Let us turn to the quantitative analysis of the phenomenon. In order to simplify the quantitative analysis, let us consider instead of the real incident beam its model, which is represented by a cylinder whose axis coincides with the $z^{(i)}$ axis, and assume that the electromagnetic field and, as a consequence, $\mathbf{g}_{\parallel}^{(ii)}(\mathbf{r})$ exist only on the cylinder's surface. In this case the family of curves, which describes the distribution of the vector $\mathbf{g}_{\parallel,p}^{(ii)}(\mathbf{r})$ on every $\Pi(z^{(i)})$, is replaced by a single curve. Next, for the illustrative purposes, let us consider the square cylinder as the incident beam's model; such a beam will be called the symbolic one. The characteristics of the symbolic beam will be denoted by underlined letters. The red sides of the square in Fig. 5(a) depict the cross section of this beam in the region of $z^{(i)}$ where $-\mathcal{X}^{(i)}(z^{(i)}) > \underline{b}$, \underline{b} being the length of every side.

Let us denote by $\underline{\zeta}^{(ii)}$ the value of the planar LM *pul* of the symbolic incident beam that is confined in every beam's side. The red arrows in Fig. 5(a) point out the directions of these momenta. TLMs of the symbolic beam are located on the horizontal sides of the square cylinder.

TLM *pul* of the symbolic beam $\underline{\sigma}_y^{(ii)}(z^{(i)})$ can easily be calculated. Its value depends on the difference $|\mathcal{X}^{(i)}(z^{(i)})| - \underline{b}$. The black thick lines I and II in Fig. 5(a) show two possible positions of the interface projection on $\Pi(z^{(i)})$ relative the beam's cross section. These lines represent the cases when $\mathcal{X}^{(i)}(z^{(i)}) < -\underline{b}$ and $|\mathcal{X}^{(i)}(z^{(i)})| < \underline{b}$, respectively. The line I does not intersect the red square; in this case $\underline{\sigma}_y^{(ii)}(z^{(i)}) = 0$, as TLMs confined in the upper and lower sides of the symbolic beam's cross section compensate each others. The line II intersects the red square, what means that the interface cuts the lower horizontal side in the symbolic beam's cross section. In this case $\underline{\sigma}_y^{(ii)}(z^{(i)}) = \underline{\zeta}^{(ii)}$, as TLM confined in the upper side of the beam's cross section is not compensated by TLM confined in its lower side. Finally, when $\mathcal{X}^{(i)}(z^{(i)}) > \underline{b}$, the symbolic incident beam does not exist. Hence,

$$\underline{G}_y^{(ii)} = \underline{\zeta}^{(ii)} \underline{D}_z^{(i)}, \quad (C5)$$

where $\underline{D}_z^{(i)}$ is the length of the uncompensated upper side of the symbolic incident beam; see the solid segment of the red line in Fig. 6, where the projections of the symbolic beams on the plane of incidence are shown. It is seen from this figure that $\underline{D}_z^{(i)} = \underline{b} \tan \theta^{(i)}$. As for the value of $\underline{\zeta}^{(ii)}$, it is

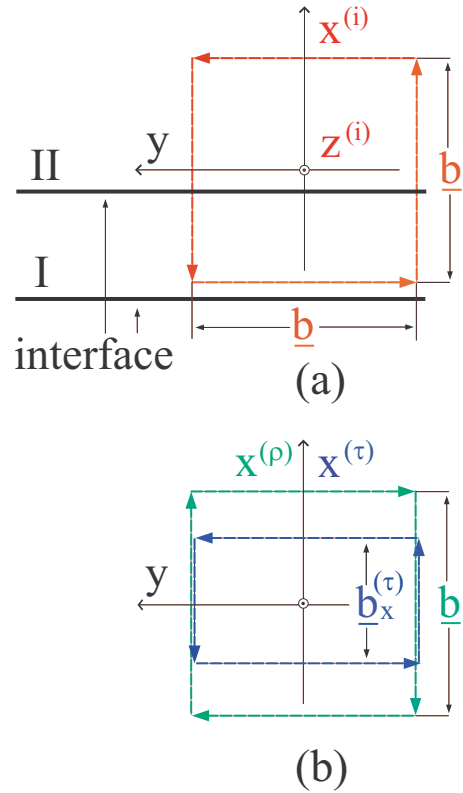


FIG. 5. The cross section of the incident symbolic beam and possible positions of the interface in it (a); the cross sections of the secondary symbolic beams (b). $n^{(1)} > n^{(2)}$, $\theta^{(i)} < \theta^{(iC)}$.

evidently related to the $[yx]$ part of IOAM *pul* of the symbolic incident beam $\underline{I}_{[yx]}^{(ii)}$ by $\underline{\zeta}^{(ii)} = \underline{I}_{[yx]}^{(ii)} / \underline{b}$. Substituting the above expressions for $\underline{\zeta}^{(ii)}$ and $\underline{D}_z^{(i)}$ into the right-hand side of Eq. (C5) we get the following relation:

$$\underline{G}_y^{(ii)} = \tan \theta^{(i)} \underline{I}_{[yx]}^{(ii)}. \quad (C6)$$

This relation is similar to the one between $G_{\parallel,y}^{(ii,S)}$ and $\underline{I}_{\parallel,[yx]}^{(ii)}$ given by Eq. (88).

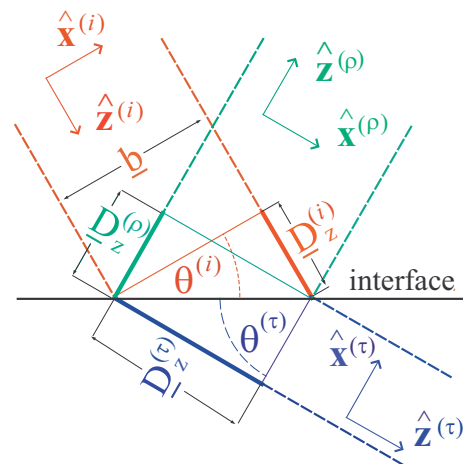


FIG. 6. The projections of the symbolic beams onto the plane of incidence. $n^{(1)} > n^{(2)}$, $\theta^{(i)} < \theta^{(iC)}$.

Let us proceed to the analysis of TLMs of the symbolic reflected and transmitted beams; the latter will be considered in the partial-reflection regime. The cross sections of the secondary beams, which are shown in Fig. 5(b), can be obtained by means of Snell's law. The $x^{(\rho)}$ and $x^{(\tau)}$ dimensions of the symbolic reflected and transmitted beams are as follows: $\underline{b}_x^{(\rho)} = \underline{b}$, while $\underline{b}_x^{(\tau)} = \underline{b}/\zeta^{(\tau)}$. The green and blue arrows in Fig. 5(b) point out the directions of the planar LMs in the symbolic reflected and transmitted beams, respectively. Note that the direction of the former vector is reverse relative to the direction of the planar LM of the symbolic incident beam; this effect will be discussed later.

The value of TLM *pul* of the symbolic secondary beam, which is confined in the upper or lower beam's side, will be denoted by $\underline{\zeta}^{(\alpha\alpha)}$. The relation between $\underline{\zeta}^{(\alpha\alpha)}$ and the magnitudes of the IOAM-dependent STLM of the symbolic secondary beam $\underline{\dot{G}}_y^{(\alpha\alpha)}$ can be obtained in the same way in which the relation (C5) has been obtained. It is as follows:

$$|\underline{\dot{G}}_y^{(\alpha\alpha)}| = |\underline{\zeta}^{(\alpha\alpha)}| \underline{D}_z^{(\alpha)}, \quad (\text{C7})$$

where $\underline{D}_z^{(\alpha)}$ is the length of the uncompensated upper or lower side of the symbolic secondary beam, see the green or blue solid segment of the respective line in Fig. 6. It can be seen that $\underline{D}_z^{(\alpha)} = (\sin \theta^{(\alpha)} / \sin \theta^{(i)}) \underline{D}_z^{(i)} = (n^{(1)} / n^{(\alpha)}) \underline{D}_z^{(i)}$. As for the relationship between $\underline{\zeta}^{(ii)}$ and $\underline{\zeta}^{(\alpha\alpha)}$, it can be obtained by means of Fresnel's law; this relationship is as follows: $\underline{\zeta}^{(\alpha\alpha)} = (n^{(1)} / n^{(\alpha)}) \underline{Q}^{(\alpha)} \underline{\zeta}^{(ii)}$. Substituting the above expressions for $\underline{D}_z^{(\alpha)}$ and $\underline{\zeta}^{(\alpha\alpha)}$ into the right-hand side of Eq. (C7) and

taking into account Eq. (C5) we get the following relation between the magnitudes of the IOAM-dependent STLMs of the symbolic incident and secondary beams:

$$|\underline{\dot{G}}_y^{(\alpha\alpha)}| = \frac{\epsilon^{(1)}}{\epsilon^{(\alpha)}} \underline{Q}^{(\alpha)} |\underline{G}_y^{(ii)}|. \quad (\text{C8})$$

The relation (C8) is similar to the relation between the magnitudes of the IOAM-dependent STLMs of the real, beams which can be obtained on the basis of Eqs. (64) and (88).

As for the signs of $\underline{G}_y^{(\rho\rho)}$ and $\underline{\dot{G}}_y^{(\tau\tau)}$, it will be shown below that both are opposite to the sign of $\underline{G}_y^{(ii)}$, whereas the reasons for the signs' changes are different for the processes of reflection and transmission.

The interface cuts the lower part of the reflected beam, like that of the incident beam. The signs of $\underline{G}_y^{(\rho\rho)}$ and $\underline{G}_y^{(ii)}$ are opposite because the directions of TLMs in the upper (lower) sides of the reflected and incident symbolic beams are opposite; compare the directions of the green and red horizontal arrows in Fig. 5. The change of the sign takes place because the upper side of the incident beam transforms into the lower side of the reflected beam and vice versa; see Fig. 6.

Unlike in the case of reflection, the upper (lower) side of the incident beam transforms into the same side of the transmitted beam; see Fig. 6. Hence, the directions of TLMs in the upper (lower) sides of the symbolic transmitted and incident beams are the same; compare the directions of the blue and red horizontal arrows in Fig. 5. However, the interface cuts the upper part of the transmitted beam, unlike that of the incident one.

-
- [1] J. D. Jackson, *Classical Electrodynamics*, 2nd ed. (Wiley, New York, 1976).
- [2] A. Wiegrefe, *Ann. Phys.* **350**, 465 (1914).
- [3] F. I. Fedorov, *Dokl. Akad. Nauk SSSR* **105**, 465 (1955).
- [4] N. Kristoffel, *Acta Comment. Univ. Tartu* **42**, 94 (1956).
- [5] O. C. Beauregard, *Phys. Rev.* **139**, B1443 (1965).
- [6] C. Imbert, *Phys. Rev. D* **5**, 787 (1972).
- [7] F. I. Fedorov, *Zh. Prikl. Spektrosk.* **27**, 580 (1977) [*J. Appl. Spectrosc.* **27**, 1236 (1977)].
- [8] V. G. Fedoseyev, *Opt. Spektrosk.* **62**, 119 (1987).
- [9] V. V. Filippov, *Zh. Prikl. Spektrosk.* **47**, 500 (1987) [*J. Appl. Spectrosc.* **47**, 971 (1987)].
- [10] L. Allen, M. W. Beijersbergen, R. J. C. Spreeuw, and J. P. Woerdman, *Phys. Rev. A* **45**, 8185 (1992).
- [11] *The Angular Momentum of Light*, edited by D. L. Andrews and M. Babiker (Cambridge University Press, Cambridge, 2013).
- [12] S. M. Barnett, M. Babiker, and M. J. Padgett, *Philos. Trans. R. Soc. A* **375**, 20150444 (2017).
- [13] M. J. Padgett, *Opt. Express* **25**, 11265 (2017).
- [14] V. G. Fedoseyev, *J. Phys. A: Math. Gen.* **21**, 2045 (1988).
- [15] V. G. Fedoseyev, *J. Opt.* **15**, 014017 (2013).
- [16] K. Y. Bliokh and A. Aiello, *J. Opt.* **15**, 014001 (2013).
- [17] I. Brevik, *Phys. Rep.* **52**, 133 (1979).
- [18] R. N. C. Pfeifer, T. A. Nieminen, N. R. Heckenberg, and H. Rubinsztein-Dunlop, *Rev. Mod. Phys.* **79**, 1197 (2007).
- [19] S. M. Barnett and R. Loudon, *Philos. Trans. R. Soc. A* **368**, 927 (2010).
- [20] B. A. Kemp, *J. Appl. Phys.* **109**, 111101 (2011).
- [21] Strictly speaking, the dimensions of the incident beam should be characterized by two parameters, $b_x^{(i)}$ and b_y . One parameter b is used in the main part of the paper for the sake of simplicity; it needs to be considered as the mean value of $b_x^{(i)}$ and b_y .
- [22] "The regular region of $\theta^{(i)}$ " means that $\theta^{(i)}$ is not close to $\theta^{(ic)}$ or to the Brewster angle in the case of $\hat{\mathbf{x}}^{(i)}$ polarization of the incident beam.
- [23] V. G. Fedoseyev, *Opt. Commun.* **193**, 9 (2001).
- [24] V. G. Fedoseyev, *Opt. Spektrosk.* **71**, 992 (1991) [*Opt. Spectrosc. (USSR)* **71**, 570 (1991)].
- [25] K. Y. Bliokh and Y. P. Bliokh, *Phys. Rev. Lett.* **96**, 073903 (2006); *Phys. Rev. E* **75**, 066609 (2007).
- [26] V. G. Fedoseyev, *Transactions of the Institute of Physics of the Estonian Acad. Sci.* **64**, 189 (1989) (in Russian).
- [27] A. Ya. Bekshaev and M. S. Soskin, *Opt. Commun.* **271**, 332 (2007).
- [28] M. V. Berry, *J. Opt. A* **11**, 094001 (2009).
- [29] Ch. F. Li, *Phys. Rev. A* **80**, 063814 (2009).
- [30] K. Y. Bliokh, M. A. Alonso, E. A. Ostrovskaya, and A. Aiello, *Phys. Rev. A* **82**, 063825 (2010).
- [31] Zh. Xiao, H. Luo, and Sh. Wen, *Phys. Rev. A* **85**, 053822 (2012).
- [32] A. Bekshaev, K. Y. Bliokh, and M. S. Soskin, *J. Opt.* **13**, 053001 (2011).
- [33] A. Aiello and J. P. Woerdman, *Opt. Lett.* **33**, 1437 (2008).
- [34] V. G. Fedoseyev, *Opt. Commun.* **282**, 1247 (2009).

- [35] K. Y. Bliokh, I. V. Shadrivov, and Y. S. Kivshar, *Opt. Lett.* **34**, 389 (2009).
- [36] M. Merano, N. Hermosa, J. P. Woerdman, and A. Aiello, *Phys. Rev. A* **82**, 023817 (2010).
- [37] In view of that, the prism $\vec{\mathcal{P}}^{(aa')}$ can be replaced with the respective half space.
- [38] Note that the relation (94) between $G_{\perp,y}^{(1)}$ and $G_{\perp,y}^{(2)}$ directly follows from Eq. (77) and the boundary conditions for the x and y components of the vector $\mathbf{E}(\mathbf{r})$ on the interface.
- [39] U. Hosten and P. Kwiat, *Science* **319**, 787 (2008).
- [40] V. G. Fedoseyev, *J. Opt.* **13**, 064025 (2011).
- [41] M. Onoda, S. Murakami, and N. Nagaosa, *Phys. Rev. Lett.* **93**, 083901 (2004); *Phys. Rev. E* **74**, 066610 (2006).
- [42] M. R. Dennis and J. B. Götte, *Phys. Rev. Lett.* **109**, 183903 (2012).
- [43] J. H. Hannay and J. F. Nye, *J. Opt.* **15**, 014008 (2013).
- [44] W. Löffler, J. F. Nye, and J. H. Hannay, *J. Opt.* **16**, 085703 (2014).
- [45] S. M. Barnett, *Phys. Rev. Lett.* **104**, 070401 (2010).